Controlling Morphology and Its Effects on the Thermoelectric Properties of $SnSe_2$ Nanostructured Thin Films

By

Maroosha Farid

School of Chemical and Materials Engineering

National University of Sciences and Technology

Year 2021

Controlling Morphology and Its Effects on the Thermoelectric Properties of $SnSe_2$ Nanostructured Thin Films

Name: Maroosha Farid

Reg.No: MSE-12-00000238343

This thesis is submitted as a partial fulfillment of the requirements for the degree of

MS in (Materials & Surface Engineering)

Supervisor Name: Dr. Muhammad Siyar

School of Chemical and Materials Engineering (SCME)

National University of Sciences and Technology (NUST)

H-12 Islamabad, Pakistan

August, 2021

DEDICATION

I dedicate this thesis to my loving and supportive father, my beloved mother and teachers.

Acknowledgement

All praises are to **Allah**, the Merciful and the All Beneficent, WHO granted me the wisdom and passion to execute my research work.

I would first like to thank my supervisor, **Dr. Muhammad Siyar**, whose expertise was invaluable in formulating the research questions and methodology. His insightful feedback pushed me to sharpen my thinking and brought my work to a good level. I would also like to thank my GEC members **Dr. Zakir Hussain**, **Dr Iftikhar. Hussain**. **Gul** and **Dr. Amna Safdar** for their constant support, advice, and valuable comments at every stage of my research work. In addition, I would like to acknowledge **Dr. Amir Azam Khan,** Principal SCME, NUST for his sincere support and guidance towards quality research work.

I would express my deep gratitude to **Haad Khan** and **Maryam Ali** for their continuous support and motivation which helped me a lot to conclude my research work.

The last but not the least, I acknowledge all the faculty members, non-teaching staff and my research colleagues who supported me throughout my thesis work.

Abstract

In this decade thermoelectric investigations of the layered structured of tin selenide (SnSe) has been carried out in more details to explore its great thermoelectric potential. It is found recently that SnSe has high efficiency and environmentally benign nature, free of toxic elements such as Pb and Te. Tin diselenide is another important chalcogenide structure from the same family but till now its thermoelectric properties are not that much explored. Due to its layered type of nature, we expect that its morphology may have profound effect on its thermal and electronic transport properties. Hence we have tried to synthesis SnSe2 structure in different morphological forms via solvothermal synthesis mechanism. These various morphologies of the structure were obtained by varying different reaction parameters such as time and temperature. The thermoelectric investigations on the various morphologies of the snse2 suggest that by modifying morphology of the SnSe2 structure thermoelectric properties may be prominently affected. The peak power factor we have obtained for the flower like morphology of the snSe2 was 0.69 $\mu Wm^{-1}K^{-2}$, which was synthesized at 575 K of reaction temperature.

Table of contents

List of figures

List of tables

Chapter 1

Introduction

Currently the world is facing many challenges related to the supply of energy and its consumption. The green energy is taking center of attention due to its environmentally safe nature. The worldwide value of the oil is increasing day by day with high prices. All the problems are driving the requirement to use the energy resources in more beneficial way. Some new technologies are under tremendous progress e.g., auto mobile engines and transmissions to increase the vehicle fuel efficiency. In these technologies there is an important issue that in normal fuel engine, it has 34% of efficiency and 66% of the total fuel cost is lost in the form of waste heat. Whereas in case of combustion engine wasted fuel energy rate is 40% and only 25% efficiency and other 30% is used for engine coolant, 5% is waste in the friction resistance [1, 2].

Now days, the fossil fuels are the main source of electrical energy generation. Fossil fuels contain carbon and were found as a consequence of geological procedure from the remains of organic matter produced by photosynthesis hundreds of years ago. In almost every industrial process unit the energy utilized is partly wasted in form a waste heat and leads to affect the green planet environment in many ways [3]. All these problems are motivating the demand of finding more convenient energy generation.

1.1 Renewable Energy Demand

The world energy statistic is regularly published by International renewable energy agency (IRENA). Figure 1.1 shows the energy consumption by region which shows that the growth will take place outside the Organization for economic co-operation and development (OECD) region. The developed world is basically the western nations where the energy consumption is relatively a flat line. The vast majority growth is under developing world. From 1995 to 2035 the growth takes place outside the OECD region.

The major finding concludes that the energy consumption by world will exceed from 18 billion toe in the year 2035.

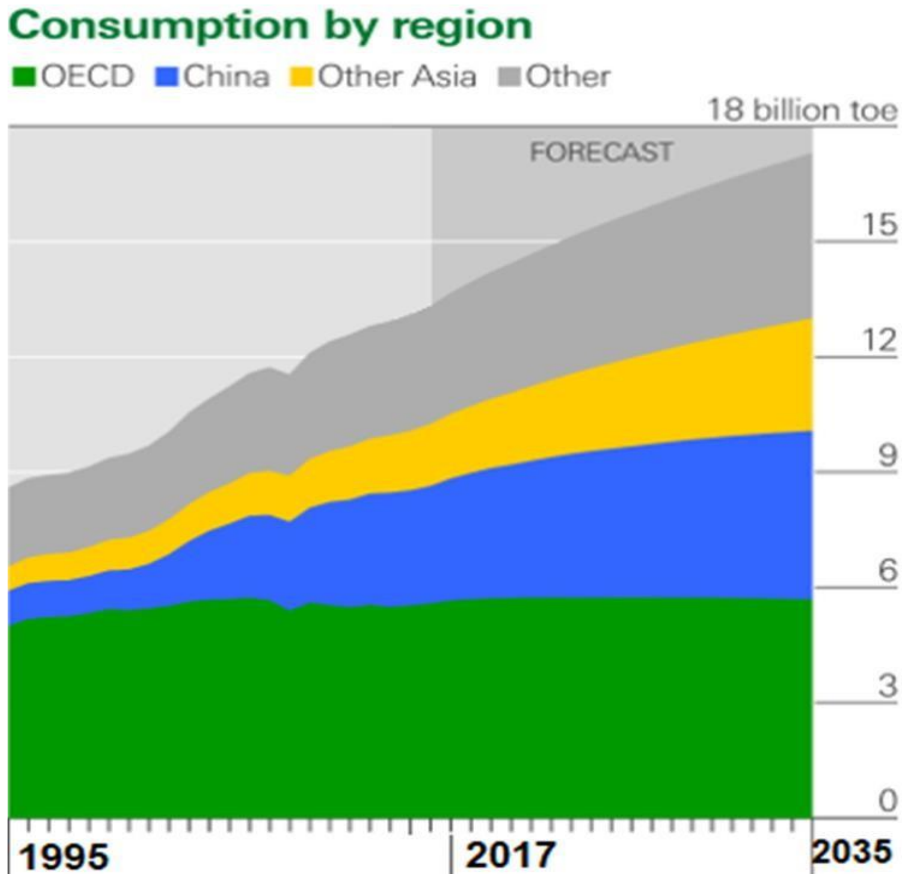

Figure 1.1: Energy consumption by region

Fig shows the volume growth by fuel according to the IRENA from 1994 to 2035. Coal, gas and oil are the most consumed fuels and from 2017 to 2035 while renewables, hydroelectricity and nuclear power are expected to provide half of the overall growth in next twenty years.

1.2 Thermoelectric (TE) Materials

The demand of other resources of energy is increasing rapidly for the entire world. To fulfill the need of global energy demand, renewables have an intensified way towards the power generation. Alternative energy sources decrease the negative impact on the environment. Improvement to the current energy supply must originate from the diverse

set of renewable energy sources like solar, wind, biomass and others. Another useful source to generate electricity from heat is to use TE materials [6]. Thermoelectric (TE) energy is basically a direct conversion of waste heat into electrical energy. A thermoelectric material does not have any moving parts, and the waste heat is directly converted into electrical energy and solid-state cooling. The heat can be generated from the burning of fossil fuels, (e.g. combustion, chemical reactions, nuclear decay). Thermoelectric materials have great potential for mobiles and distributed heat harvesting, such as vehicle exhaust heat recovery. Thermoelectric phenomenon, involve the presence of electronic and phononic transport. The efficiency of thermoelectric materials is characterized by the figure of merit (ZT) [4, 5].

1.3 Application of TE Materials

Thermoelectricity is obtained through the conversion waste heat energy into electrical energy directly. There are many applications of thermoelectric devices that can cover a wide range of products [7]. The developments of new materials that are more efficient are going to expand the area of thermoelectric energy applications for thermoelectric generators and coolers. Many researches have been directed to discover highly efficient TE materials, mostly nanostructured [8]. The important application of thermoelectric in power generators, as TEGs, is power harvester. It can transfer heat energy in the form of electricity, for example, solar energy into electricity [11]. According to the research, in the process of configuration 60% energy is lost in the form of waste heat [9]. The effect of energy loss is high, has lower efficiency and also has a negative impact on the environment. TE devices in the automotive industry can provide some unique features and these features are divided into two parts i.e. Peltier effect, which is basically focused on conversion of electricity into cooling; and Seebeck effect which converts waste heat into useful energy in the form of electricity. These approaches are not only highly efficient but also are not hazardous to the environment [10].

Human body can also be used as a source of heat for TE applications as the human body produces constant and stable heat which can be used for precise set of applications. Human body has the capacity to release up to 100 watts of heat [12]. There are certain electronic devices that have already been developed that can be used for converting the

heat generated by human body into useful work. Citizen watches with their eco-drive technology, use the heat from human body as the main power source for running their wrist watches. Similarly, Seiko and Dyson TE are also working along the same lines where heat from the body is used to charge the integrated battery. Research is ongoing when it comes to using human body as means to charge one's mobile phone [13].

1.4 Thermoelectricity

When a TE material is exposed to heat energy, it can use that form of energy to convert it into electrical energy. When heat is applied, charge carriers diffuse from hot side towards the cold side and as a result of moving charge carriers, electric current is generated [14]. In TE devices due to temperature gradient that exists between the two ends of the module, potential difference is generate which gives rise to generation of electrical voltage. The phenomenon is termed as Seebeck Effect. Conversely, when electric voltage is applied to a TE device, it can use that voltage to provide a specified temperature which can be termed as cooling as well. This phenomenon is call TE cooling or Peltier effect [15].

1.4.1 Seebeck Effect

In 1821 Thomson Johann Seebeck discovered the thermoelectric effect. If two conductors or semiconductors are linked together and one side of the conductor is hot and other side is cold, the potential difference can cause the electric charge to flow and as a result, generate electricity. This occurs as a result of the temperature gradient (oT) that exists between the two dissimilar conductors [16]. This concept is termed as Seebeck effect. From the hot side towards the cold side, maximum charge carriers are diverged thermally. As a result of this divergence, electric field is generated, which brings out to accumulation and the diffusion of charges can be balanced as shown in fig 1.3[21]. Seebeck coefficient is basically a relationship between electrical voltage and temperature difference [22]. And the equation can be represented as:

$$\mathbf{S} = \frac{\Delta V}{\Delta T}$$

S = Seebeck coefficient

ΔV = Electric field

ΔT = Temperature gradient

For p-type material the Seebeck coefficient is positive and for n-type material the Seebeck coefficient is negative [23].

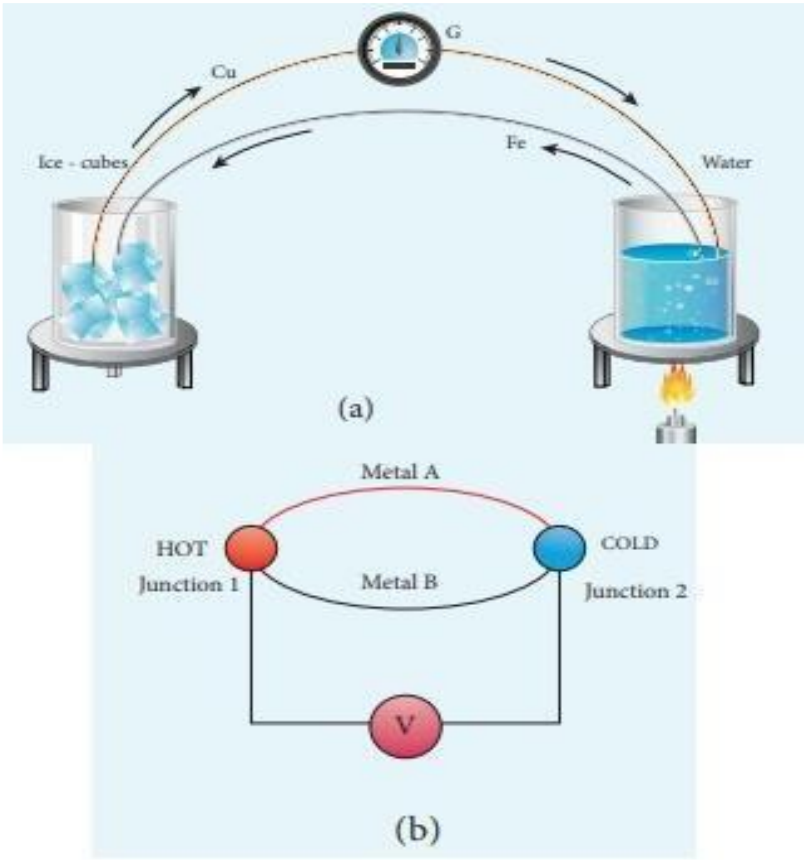

Fig 1.2: Seebeck effect

1.4.2 Peltier Effect

Peltier effect is the reverse phenomena of Seebeck effect. A French physicist named Jean Charles Athanase, discovered in 1834 that in the existence of temperature difference (heating or cooling), electric field is initiated at two different sides of conductors or semiconductors [24]. When electric field is initiated and it flows through the circuit, at the junction, heat may be added or removed between the two materials [25]. Peltier effect is a relationship between heating, cooling and the electric current

when it circulates in the circuit. Peltier effect can be expressed through the following equation [26]:

$$\Pi = \overline{I}$$

M = Peltier coefficient

I = Absorb heat

QM = Applied Heat

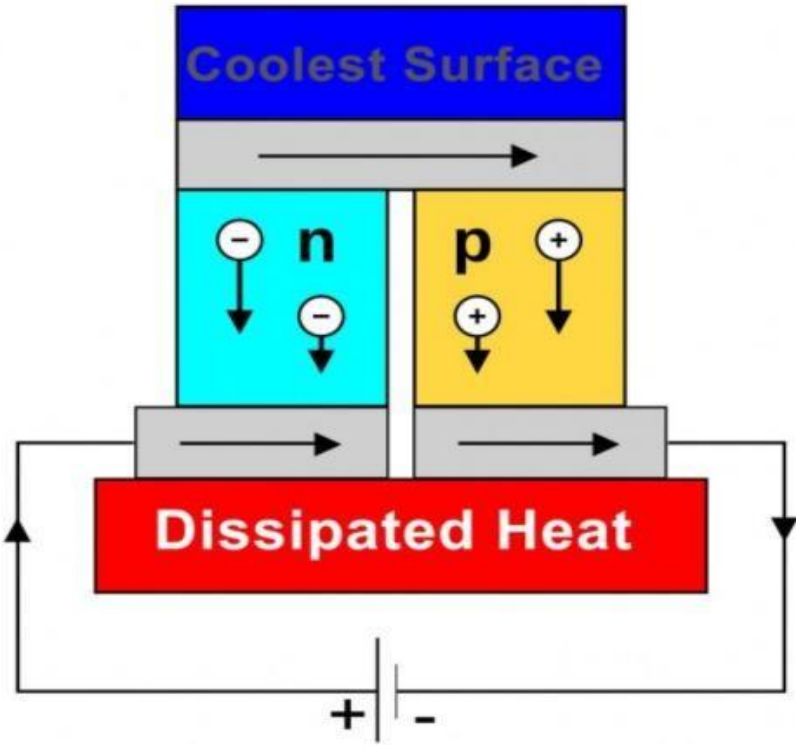

Fig 1.3: Peltier effect

1.4.3 Thomson Effect:

In 1854 William Thomson discovered that for a single material, if heated, the heat flows from hot end to the cold end but it also gives rise to movement of charge carriers, resulting in the formation of electric current. This phenomenon is termed as Thomson effect [27]. Thomson effect shows the direct relationship between Peltier effect of

cooling and Seebeck effect of heating. Thomson effect is defined as, when electric current passes through a single material, the heat generated produces a temperature gradient along the length of the material [28]. Thomson effect is expressed as

$dQ = \beta I dT$

Where

dQ = rate of heat generation

β = Thomson coefficient

I = Applied current

dT = Temperature gradient

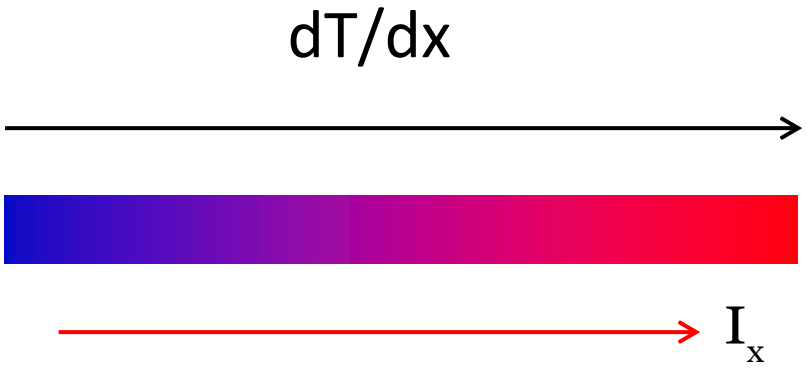

Fig 1.4: schematic diagram of Thomson effect

1.5 Figure of Merit (ZT)

Figure of merit of the thermoelectric materials can be defined as the performance parameter; the higher ZT, higher will be the efficiency of a material [29]. It can be represented using the following equations:

$$\mathbf{ZT} = \frac{S^2}{\rho K} T$$

$$\sigma = \frac{1}{\rho}$$

$$\mathbf{ZT} = \frac{S^2 \sigma}{K} T$$

S = Seebeck coefficient, T= absolute temperature, ρ = electrical resistivity, k = thermal conductivity, σ = electrical conductivity

ZT is dimensionless figure of merit and figure of merit is basically dependent on temperature and also it is derived from temperature dependent material properties [30]. For the maximum value of ZT Seebeck coefficient and electrical conductivity must be high along with low thermal conductivity. Furthermore, there are two components of thermal conductivity that are $k= k_e+k_l$. If the lattice conductivity will be low then overall thermal conductivity will drop. These parameters are related to the carrier concentration and band gap structure [31].

1.6 TE Module

Thermoelectric module is based on n-type material and p-type materials. Electrons move towards one side and holes move towards the other side, when heat is applied. TE materials that have majority charge carriers in n-type and electrons are dominant in nature are termed as n-type TE materials while those with majority charge carriers in p-type or where holes are dominant are termed as the p-type TE materials [32].

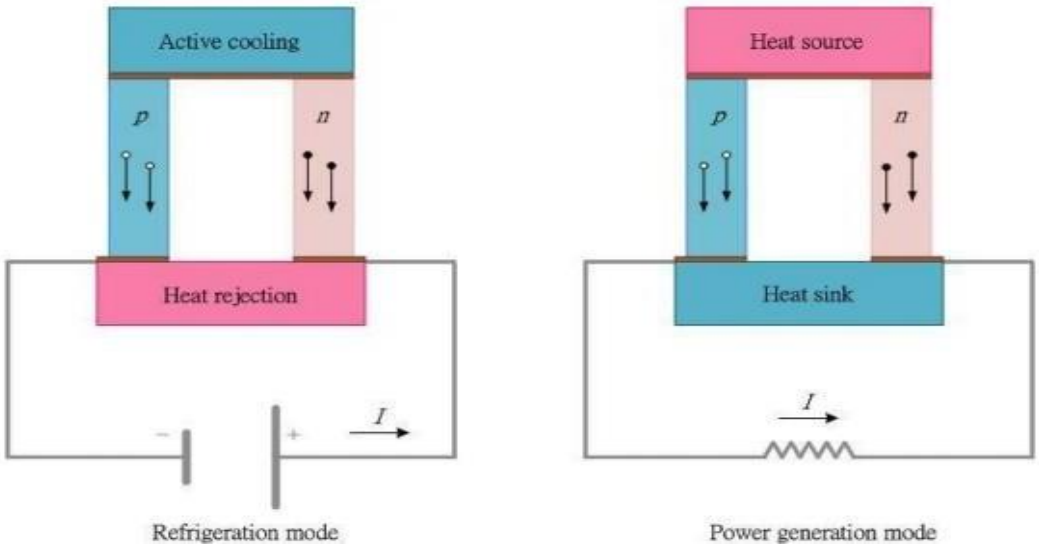

Fig 1.5: Thermoelectric couple consisting of n-type and p-type TE materials.

1.7 Material Selection Criteria:

In order to have an improved set of TE properties, a material must have a higher ZT value so in order to achieve higher TE properties; we need to achieve higher values of ZT. Fig 1.7, show the material selection criteria. The graph depicts that for semiconductors class of materials, the required properties for ZT i.e. electrical conductivity, Seebeck coefficient and thermal conductivity, all lie at a moderate value, making semiconductors the most suitable class of materials for TE research. For efficient thermoelectric materials, low thermal conductivity is required. There are two parts of thermal conductivity k_l is derived from the crystal lattice part while k_e is derived from the electronic part or charge carriers. For a TE material to have enhanced TE properties, it is important that it has a bandgap value of less than 1eV in order to achieve a better carrier concentration along with good carrier mobility [34].

Fig shows that three classes of materials; insulators, semiconductor and metals. The ZT value of insulators is low, σ is also poor but the Seebeck value is high that's why insulators are not efficient for thermoelectric applications. The metal shows the high σ, high k, and low Seebeck value and ZT value remains low. So, metals are also not much suitable for TE properties. So, we can choose semiconductors because high Seebeck low σ and low k so we can achieve high ZT [35].

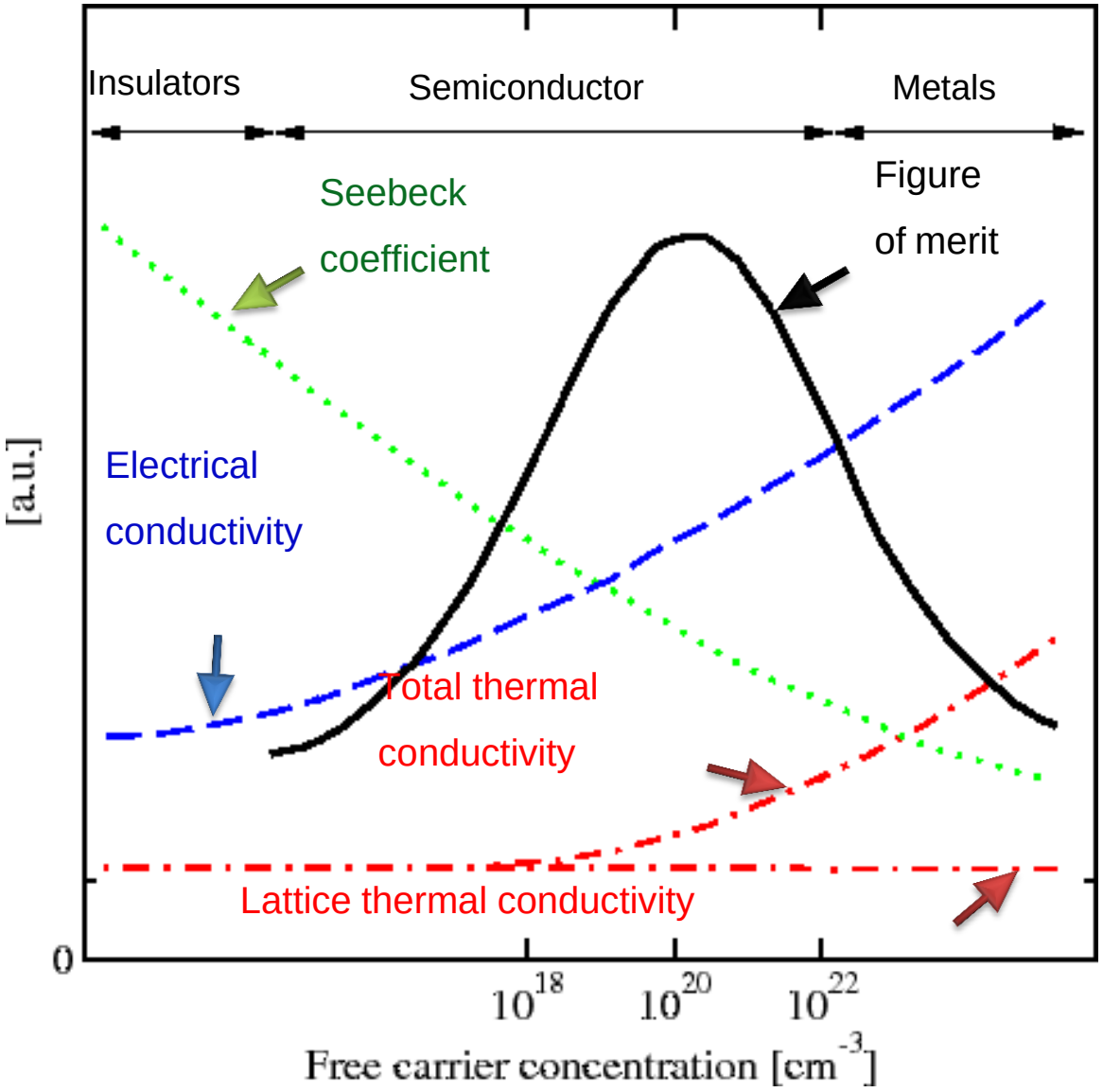

Fig 1.6: dependence of ZT on carrier concentrations

1.8 Challenges in TE Research:

In thermoelectric research there are lots of challenges. Fig 1.7 shows the figure of merit value variation between 1960 and 2016. Fig shows the TE materials divided into three parts the ZT value is less than 1and the efficiency of power conversion is 4-5%. Between 2004 and 2010, the ZT value was improved from 1 to 1.7 and the efficiency from 11% to 15% and in third part the high-performance TE materials showed a ZT value of 1.8 and an efficiency of 15% to 20%. It also shows a shift toward

chalcogenides. According to the research and graph the SnSe shows good physical and chemical properties [36].

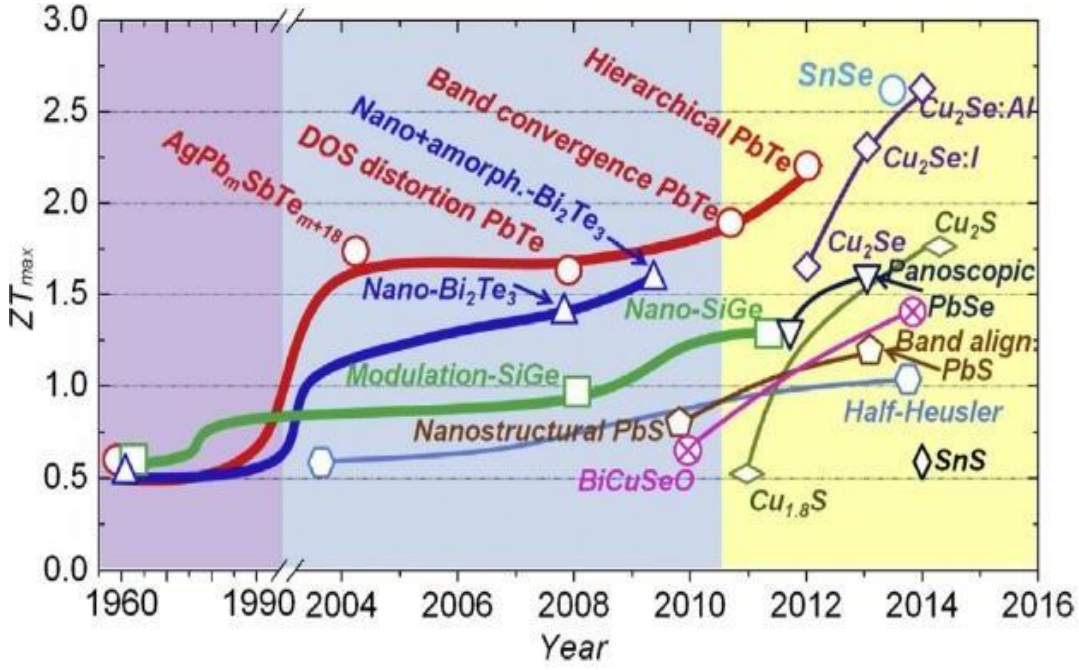

Fig 1.7: ZT value of various thermoelectric materials from year 1960 to year 2016. The latest research predicts that most of the high ZT TE structures of chalcogenides.

The figure 1.8 shows the Sn and Se are both abundant as well as low-cost materials as compared to other options. Selenides are high performance thermoelectric materials and highly efficient. Compared to the other sulfides and oxides SnSe is cheaper and environmentally friendly as well [37].

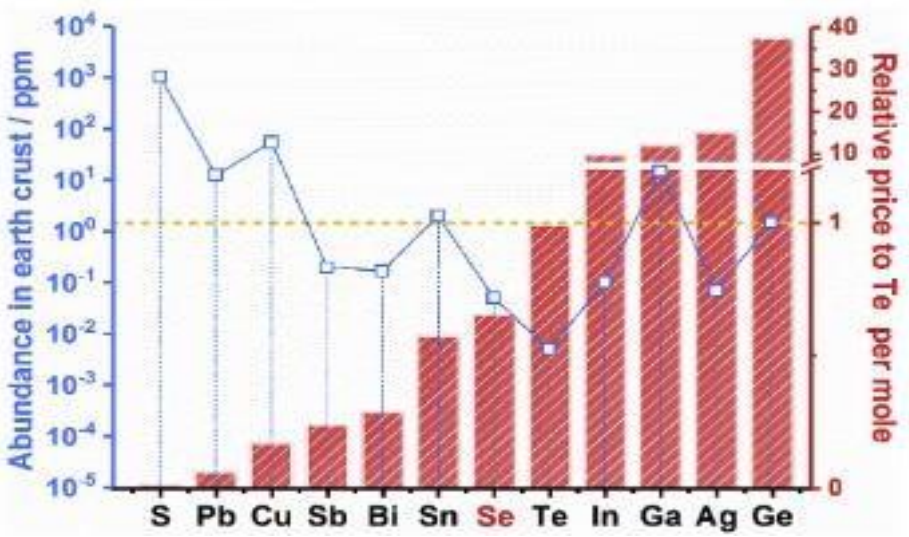

Fig 1.8 Abundance and Price of different TE materials

1.9 Advantages of TE materials:

Thermoelectric materials are most widely used as renewable energy resources. Many advantages of TE materials are as follows: the solid-state TE devices have no moving parts that are why they are more reliable and efficient. The TE devices are not like compressor-based cooling system hence the response times are faster [71]. In TE devices there is no noise as compared to the other compressor technology. Solid state TE devices can be arranged in any orientation.

Chapter 2

Literature review

In this research our major focus is how to improve thermoelectric properties of tin diselenide. There are many ideas and methods to boost the TE properties of $SnSe_2$. And some of the plans are discussed further.

2.1 Approaches to control electrical conductivity of TR materials

The electric conductivity measures the capability of the material to conduct electric current. Electrical conductivity is equal to the product carrier concentration and carrier mobility.

$$\sigma = \mu ne$$

The acceptable electrical conductivity value for TE materials is $10^{-5} S m^{-1}$. That can be achieved through high carrier mobility or high carrier concentration.

2.1.1 Carrier concentration

For enhancing the electrical conductivity of $SnSe_2$ carrier concentration plays an important role because electrical conductivity depends on carrier concentration and mobility. For good thermoelectric material, the range of carrier concentration is 10^{18} to $10^{21} cm^{-3}$ which is a desired value for achieving ideal power factor [42]. There are two individual methods to control the carrier concentration.

I. Extrinsic doping
II. Tuning intrinsic defects

The simplest way to do extrinsic doping is the alloying with the adjacent columns from periodic table. In many cases the ideal concentration is difficult to achieve, the reason behind this difficulty is solubility limit and doping capability of dopants. This is the reason why the properties displayed in theoretical study of TE materials cannot be achieved in experimental work. In addition, few complicated semiconductors consist of

two or more elements and as a result of the existence of new dopants, the solubility of the dopant becomes difficult [43].

Tuning intrinsic defects involve vacancies, interstitials, etc. to obtain the desired carrier concentration. These defects decrease the TE performance and reduce the efficiency. The carrier concentration of the defects is totally dependent on the composition of elements [42].

2.1.2 Carrier mobility

Carrier mobility is a major variable to improve electrical conductivity. Carrier mobility is an ability that tells us how fast the charge can move among the semiconductors. These are some techniques to improve the TE properties [44].

2.2 Approaches to improve Seebeck coefficient

The equation of ZT shows that the Seebeck coefficient is dominant than other variables e.g., electrical conductivity and thermal conductivity in order to obtain high figure of merit value. Improved Seebeck coefficient is more important than lowering thermal conductivity and increasing the electrical conductivity [45]. Seebeck coefficient is represented as:

$$\mathbf{s^2} = \frac{8\pi^{2}K_B^{2}}{3eh^2} m_d^* T \left(\frac{\pi}{3n}\right)$$

In this equation the variablesK_b, eh, $m^*_d$are the Boltzmann constant, carrier charge planks constant and DOS effective mass respectively [46].

2.3 Approaches to reduce thermal transport properties:

Thermal conductivity is the capability of any material or structure to pass heat at some specific temperature. The total conductivity depends on two factors that are thermal conductivity of electrons(k_{ele}) and thermal conductivity of lattice(k_{lat}) [47].

$$\mathbf{K} = k_{ele} + k_{lat}$$

To determine the thermal conductivity of electron the Wiedemann- Franz law can be applied.

$$k_{ele} = \mathbf{L}\sigma\mathbf{T}$$

L is Lorentz parameter; and the range of Lorentz parameter is 1.6 to 2.5 WΩk^{-2}. Wiedemann- Franz law states that the thermal conductivity of the electrons increases with the rise in electrical conductivity. That's why suitable TE materials and enhanced carrier concentration is essential to achieve higher ZT [48].

2.3.1 Point defects:

The reason behind introduction of point defects is to generate lattice imperfection along the length of interatomic distance. The thermal conductivity model was developed by Kelemen's and Callaway. According to them, in point defect, the phonons are scattered at shot MFP (mean free path). This is due to the local bond strain is the influence of defects. And all this is due to the scattering parameter and is expressed by equation.

$$F = \mathbf{x}\ \mathbf{(1\text{-}x)}\ [(\Delta M/M)]^2 + s\left(\frac{a_{disorder} - a_{pure}}{a_{pure}}\right)^2$$

The above equation shows that the x is doping fraction, $\Delta M/M$ is the change in atomic mass, a_{disord} , a_{pure} shows the lattice constant of pure alloy and disorder while s is elastic property [49].

2.3.2 Nano structuring

This is another strategy to decrease thermal conductivity. This strategy can be obtained from a solid solution or nano scale particles in a single phase. Nano scale particles can be obtained by bottom-up process or mechanical methods (ball milling and melt spinning). And the remaining second phase precipitations particles can be obtained through the method of solid-state solution that are highly doped and then rapidly quenched. The second phase consistency in the solid state must have no or low solubility, and in liquid phase it must be fully soluble [50].

2.4 Metal chalcogenide:

Metal chalcogenides is basically a chemical compound which contains minimum one chalcogen anion and minimum one or more electropositive element. In the group VIA, the elements present are called chalcogens [38]. The word metal chalcogenides are usually adopted for selenides, tellurides, and sulfides. Metal chalcogenides exist with different composition like binary, ternary, etc. along with different structures as well [39].

2.5 SnSe based TE materials:

SnSe based crystals are magnificent thermoelectric materials because the reported ZT value of SnSe is high (~ 2.6 ZT). The ZT value ranges from 0.1 to 0.9 when the temperature range is in between 300-773k. For higher ZT, higher temperatures are required. Tin selenide is simple in structure, stable and earth abundant material that is the reason it is chose for our TE research [52].

2.5.1 Structure of SnSe:

Another name of tin selenide is stannous selenide. It has a layered structure and belongs to the group of metal chalcogenides. Because of a low thermal conductivity and good electrical conductivity, tin selenide is included among the efficient thermoelectric materials. It has an orthorhombic structure at room temperature [53]. There are two atoms present along the b and c planes. The joining of SnSe atoms is with heteropolar bonds and it consists of a chain like zigzag planes. Every Sn atom is attached to three Se atoms. The forces present in these layers are Van der wall forces [54].

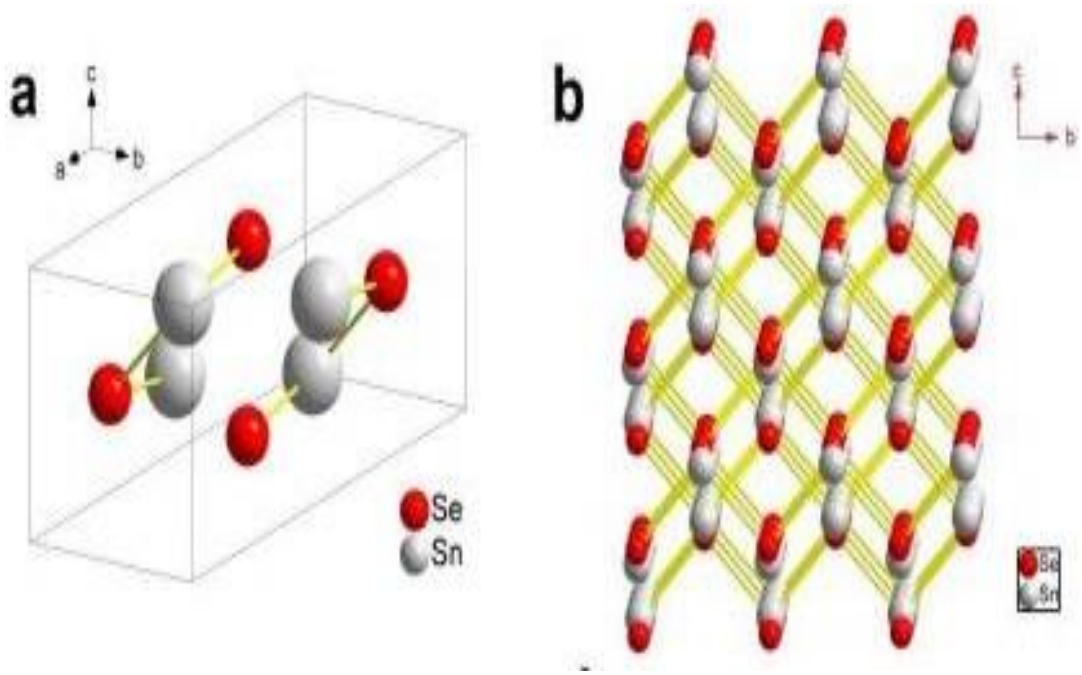

Fig 2.1: unit cell of SnSe and crystal structure

2.5.1.1 Anharmonic bonding

Anharmonicity corresponds to the lattice vibration and consequently, it affects the SnSe structure's heat transportation. The important characteristic between the Sn and Se is the anharmonic bonding between the crystal structures of SnSe. Under the light of this reasoning, SnSe has a low thermal conductivity. Fig 2.2 shows the connection between the harmonicity and anharmonicity, where Ø(r), a_o, and r are the potential energy, lattice parameter and distance between two atoms [55].

For harmonicity, when the vibrational motion of phonon is taking place, during this period, if an atom is diverging due to the force from its equilibrium position, then the force that is applied is proportional to its displacement, and the displacement in turn, is proportional to the spring constant. The harmonicity indicates balanced phonon transport. Anharmonicity is the relation between the displacement and the restoring force. When anharmonicity is high, it results in increase in phonon concentration and consequently, K_l reduces [56].

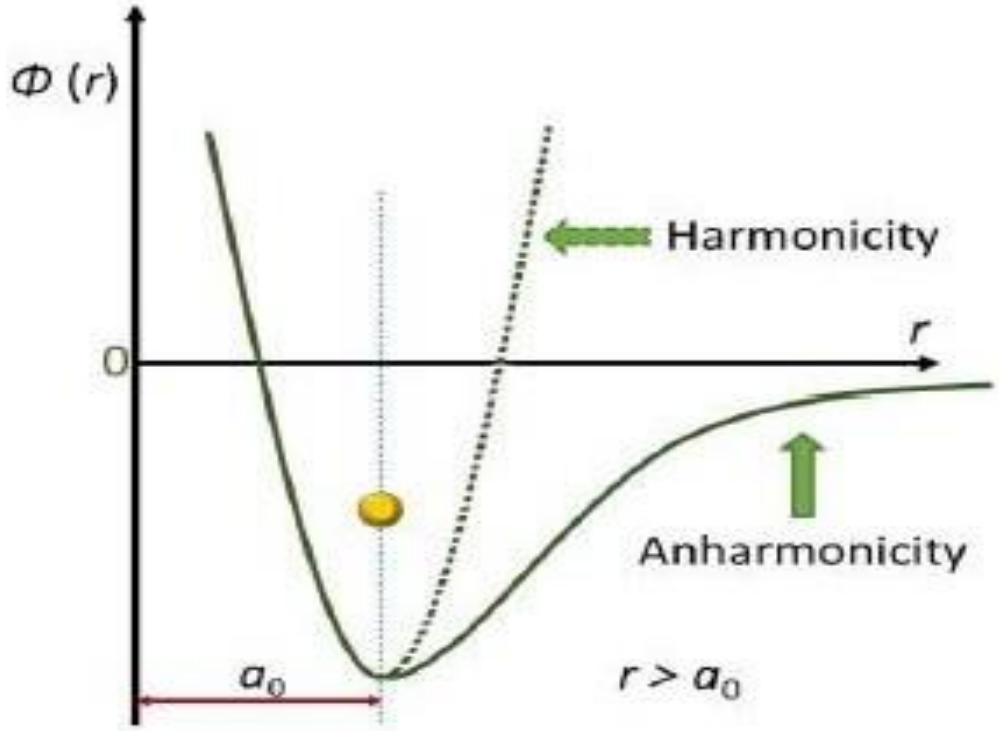

Fig 2.2: schematic diagram of harmonicity and anharmonicity

2.5.1.2 Phonons scattering effect

In polycrystalline materials SnSe, at grain boundaries lattice defect, such as dislocations, phonons scattering takes place. The phonon scattering reduces lattice thermal conductivity. The main reasons for the origination of phonon scattering in polycrystalline SnSe materials involve dislocations, precipitates, point defects and grain boundaries. At an atomic level, vacancies and substitutions, which are a part of point defects, are encountered. Dislocations and precipitates are associated with nano scale while grain boundaries are associated with sub-micro scale [57,58].

2.6 Structure of $SnSe_2$

Tin selenide also called stannous selenide and represented with the formula SnSe, is a part of metal dichalcogenides, with a close packed hexagonal structure [40]. The structural analysis can be divided into different portions e.g., phase diagram, crystal structure, mechanical properties and thermoelectric properties. As $SnSe_2$ is a family member of metal dichalcogenide semiconductor (MDCs), as mentioned above as well, and belongs to the group VI, $SnSe_2$ exhibits a layered structure and the stacking sequence is dependent on three layers of (Se-Sn-Se) which are parallel to the plane (001). There are weak van der wall forces present in each layer. The nature of $SnSe_2$ is n-type semiconductor. Every three-layered sandwich consists of tin atoms (monolayer) and packed between the monolayer of close-spaced selenium atoms [40]. Fig 2.1 shows 3.08Å is the distance between the three layers and 1.53Å is the distance between the two layers. Chalcogenides structures are performing much better as thermoelectric materials than conventional semiconductors. Snse2 is an important chalcogenide with binary layered structure owning hexagonal lattice of CdI2 type with P3m1 space group, which is used extensively in so many applications like optoelectronics and solar cells [8-10]. The chemical composition in general form of SnSe2 can be represented in MX2 form where M represents metal and X represents any chalcogenide element.

In more detail, it is similar to 2H poly type brucite structure where Se-Sn-Se two dimensional networks are formed along 001 plane. Here each packet of these three layers having closely packed Se atomic layers with centrally exists Sn atom [11].

The SnSe2 structure has Vander walls type of bonding among layers while covalent bonding among each packet. [12]. The electronic transport nature of SnSe2 is n-type with an indirect narrow band gap of around 0.9 eV. Due to narrow band gap chalcogenide structure it is widely applied for so many applications like, gas sensors, optoelectronics solid state devices and micro transistors.

Due to its layered type of nature, we expect that its morphology may have profound effect on its thermal and electronic transport properties.

Various studies are available in literature regarding the synthesis of SnSe2 structure in different morphological forms. And it was found that various reaction parameters can

affect the morphology and structure of Snse2 [15, 16], but no one explored the effect of its structure and morphological variations on the thermoelectric properties. Hence we have tried to synthesis SnSe2 structure in different morphological forms via solvothermal synthesis mechanism. These various morphologies of the structure were obtained by varying different reaction parameters such as time and temperature. The thermoelectric investigations on the various morphologies of the snse2 suggest that by modifying morphology of the SnSe2 structure thermoelectric properties may be prominently affected.

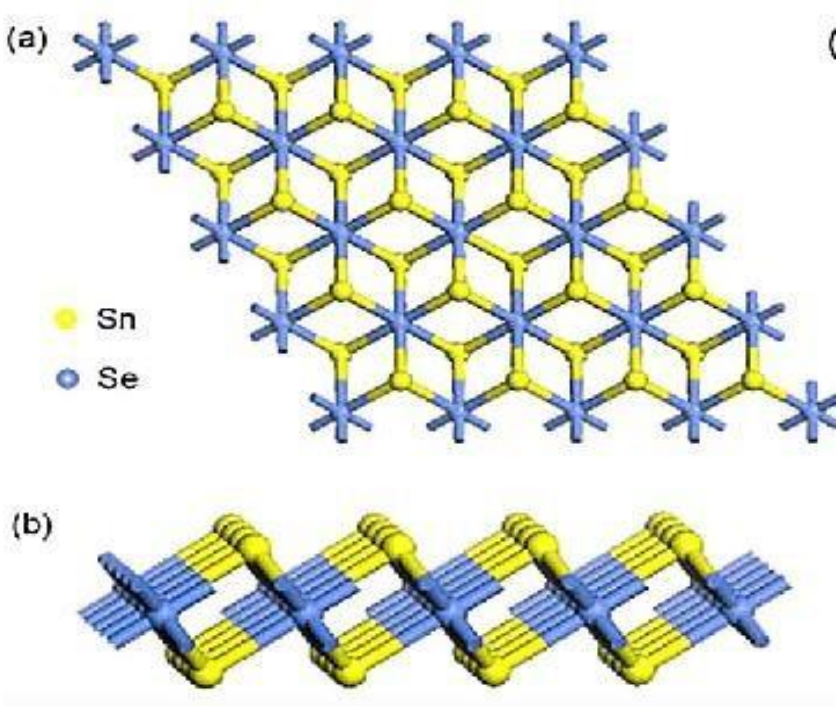

Fig 2.3: crystal structure of $SnSe_2$

2.7 Reports on Synthesis of $SnSe_2$

Dabdel Hady synthesized $SnSe_2$ thin films using the thermal evaporation method. The pressure in the vacuum is 10^{-3}Pa. Glass substrate is used for casting. Annealing time of

the film is 500k for 2h. Thermal energy band gap is measured that is enhanced from 1eV to 0.96eV [61]. D. Martinez synthesized the $SnSe_2$ and SnSe thin films by spray pyrolysis technique compounds with the ratio Sn:Se=1:1. The substrate temperature range is 275 to 400°C. The band gap of deposited film of $SnSe_2$ achieved was 1.59eV and the electrical conductivity is n-type. The annealed film then represents a bandgap of 0.81eV and it shows the p-type electrical conductivity [62].

Jewan Sharma synthesized $SnSe_2$ thin film by salinization at high temperature, the application of this paper is on phase change memory applications. He faced many problems due to selenization [63].

K. Sareetha synthesized the $SnSe_2$ thin films. The method they chose was sputtering tin followed by selenization process. The temperature for selenization is 300, 350, and 400°C. In the results, SEM shows plates-like structure. Optical band of the thin film in the range of 1.60 to 1.81 eV was achieved [64]. Enue Barrios synthesized $SnSe_2$ thin films by the heat treatment of SnSe at the temperature of 350°C. The thickness of thin film is 120 to 280nm. Thin film deposition was performed through chemical bath and as a result orthorhombic crystal structure was achieved. The band gap achieved was 0.94eV. At 430°C thin film shows n-type behavior and when heated at 530°C, it converts into p-type thin film. The applications of this research are photovoltaic and thermoelectric [65]. Hongwen Chen synthesized $SnSe_2$/CNTs. In this research work $SnSe_2$ and CNTs are combined to form a hybrid nano structure $SnSe_2$/CNTs. The structure is regular hexagonal structure with CNTs and $SnSe_2$ nano sheets. The efficient electrochemical performance of these CNTs helped them in using these in the lithium ion batteries [66].

Zhen Fang synthesized $SnSe_2$ nano sheets via a solvothermal route. Solvent is benzoyl alcohol and PVP is added as a surfactant. Benzoyl Alcohol act as a reducing agent as well as solvent and it help to develop hexagonal structure of $SnSe_2$. PVP creates the environment for Nano sheets of $SnSe_2$. The applications include in this research is photo detector and photovoltaic devices [67]. Hogwen Chen synthesized $SnSe_2$ Cu-doped nano flacks from the hydrothermal method/ technique. The obtained $SnSe_2$ structure is hexagonal layered 2-D structure and the thickness is 10-50nm. The application of this

research is to improve/enhance the electrochemical performance with the help of doping [68]. Kegao Liu synthesized $SnSe_2$ nano flacks by hydrothermal co-reduction method and the temperature used was 180°C. In this research the main focus was on the morphology and growth direction. The thickness of the nano flacks is 30-40nm and the side length is about 600-700nm [69].

Synthesized $SnSe_2$ thin films and the film is grown-up on the Al_2O_3 substrate. Pulsed laser deposition method is used to grow the films. Thin film is annealed at 400°C for 60min. The film shows the n-type semiconductor behavior. The carrier concentration is achieved from 10^{19} to 10^{20} which is in the range of acceptable value for better performing TE materials [70].

2.8 Objective of research

- Synthesis of tin diselenide ($SnSe_2$) phase pure structure using solvothermal route.
- To control the morphology of solvothermally synthesized SnSe2, by varying reaction time.
- To study the effect of morphology of $SnSe_2$ thin films on its thermal and electrical transport properties

Chapter 3

Experimental work

3.1 Material Selection

- Reactants ($SnCl_2.2H_2O$, SeO_2)
- Polyvinylpyrrolidone (PVP) present as a reducing agent, growth modifier and surface stabilizer.
- Benzoyl Alcohol ($C_6H_5CH_2OH$) as a solvent.
- Ethanol (C_2H_6O) for washing.

3.2 $SnSe_2$ Synthesis (Experimental Procedure)

We have synthesized various morphologies of SnSe2 via solvothermal synthesis route. In the detail experimental procedure, 40 ml of benzoyl alcohol was poured into a 250 ml beaker and put on to a hot plate for stirring at room temperature. After that polyvinylpyrrolidone (PVP) was added slowly up to 6 g, followed by a continuous magnetic stirring for around 8 minutes. The solution was turned transparent and apparently all the PVP was fully dissolved. Now 0.22 g $SnCl_2.2H_2O$ was added and left for 15 minutes magnetic stirring to achieve the transparent solution again. In the last 0.011 g of SeO_2 was added to the reaction and the transparent solution turned into a dark orange color. After the proper mixing of the required precursors, the reaction media was transpired into a solvothermal reactor containing a stainless steel autoclave. The reactor vessel was tightly closed and kept the setting temperature at 180 C for around 16 hours of heating time. The dark particles were obtained at the end of the solvothermal process which was washed several times with ethanol with the help of the centrifuge to remove the reaction media and obtain the pure SnSe2 particles. This washing process was repeated five to six times per sample. We have repeated the same procedure with varying the reaction time during solvothermal process as 16, 20, 24 and 48 hours for the samples M1, M2, M3 and M4 respectively.

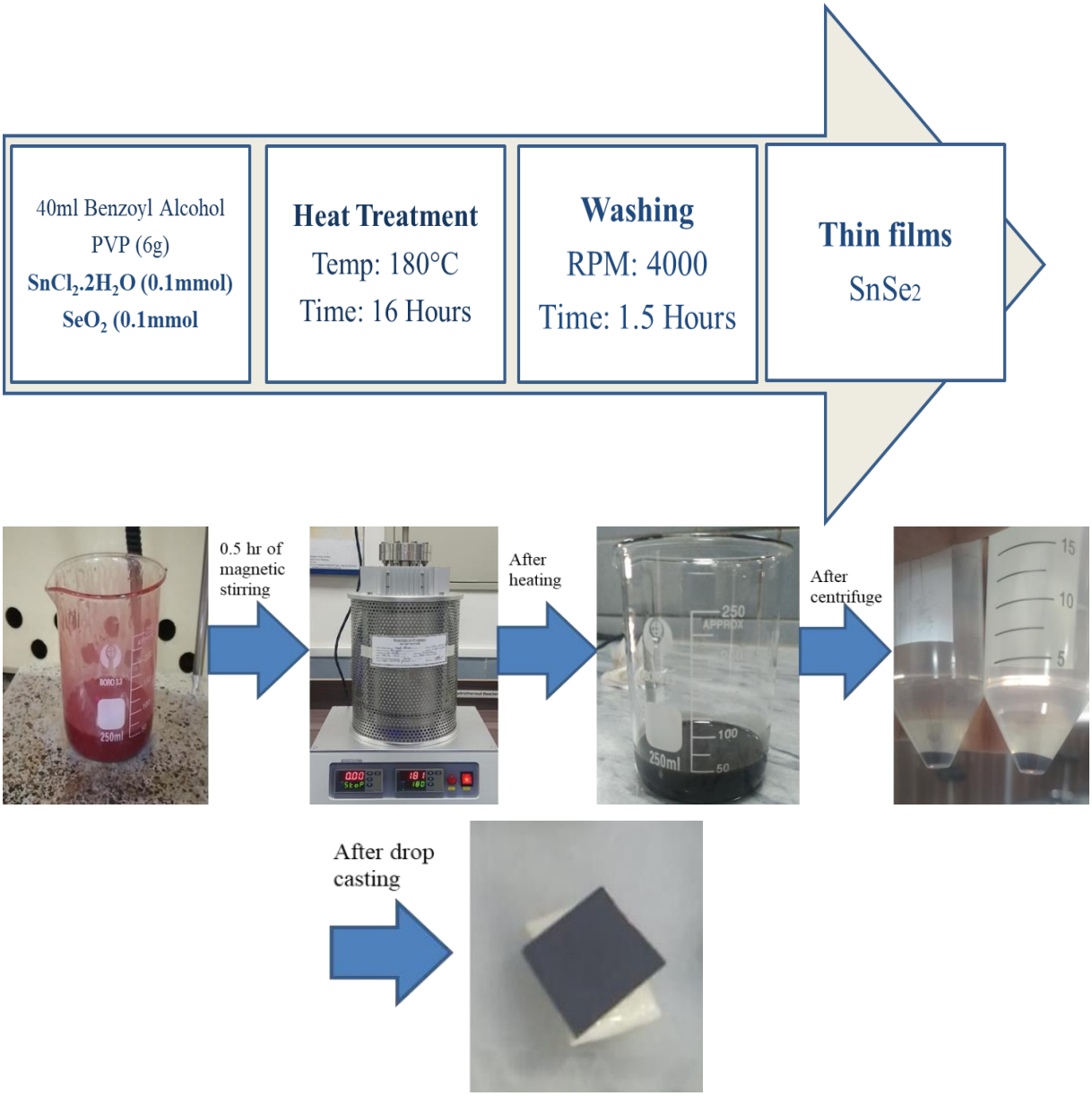

Fig 3.1: synthesis of tin diselenide

3.3 Deposition of the thin films

The resultant can then be used to be deposited as thin film on a glass substrate or silica substrate to obtain different properties. Substrate plays an important role in achieving different properties.

There are many techniques to deposit thin films e.g. vacuum thermal evaporation, electron beam evaporation, laser beam evaporation, spin coating and drop casting. We chose simple method of coating that is drop casting to obtain uniform thin films [17].

Basically, drop casting is a procedure to form a uniform thin film on a substrate. Drop casting is uncomplicated and a simpler technique than other techniques [20]. This technique is close to spin coating, but the main distinction is no spinning of substrate is required [18]. The diameter of the film and its effectiveness relies on the concentration and volume of dispersion. The major advantage of the drop casting is that there is no wastage of material during the process [19].

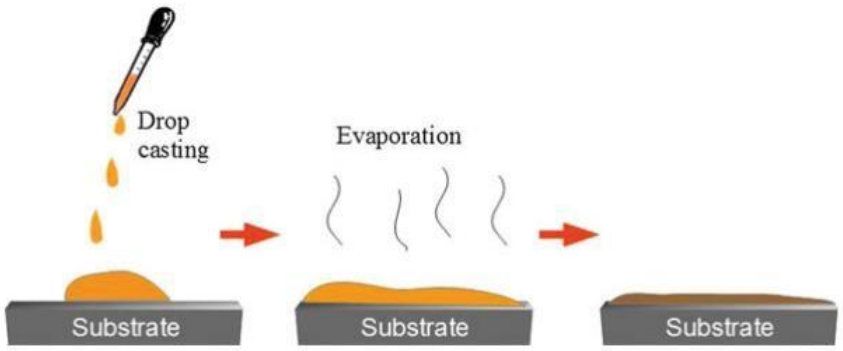

Fig 3.2: Process of Drop Casting

Thin films were drop casted on the glass substrate of SnSe2. In detail procedure, the glass slides were cut into 10 by 10 mm square type substrates with the help of a diamond cutter. These substrates were thoroughly washed with ethanol and then Sonicated for 20 minutes with the help of a sonication bath in the ethanol media to remove any impurities from the glass substrate surfaces.

Now the viscous suspension of SnSe2 nanostructure was prepared by mixing it in the

ethanol solution. The dark thick suspension obtained were drop casted with the help of micropipette on the glass substrate and air dried for few hours. The air dried thin films were heated at 80 C for 24 hours in oven to dry it completely followed by annealing in a tube furnace in the presence of N_2 media at 300 °C for 30 minute.

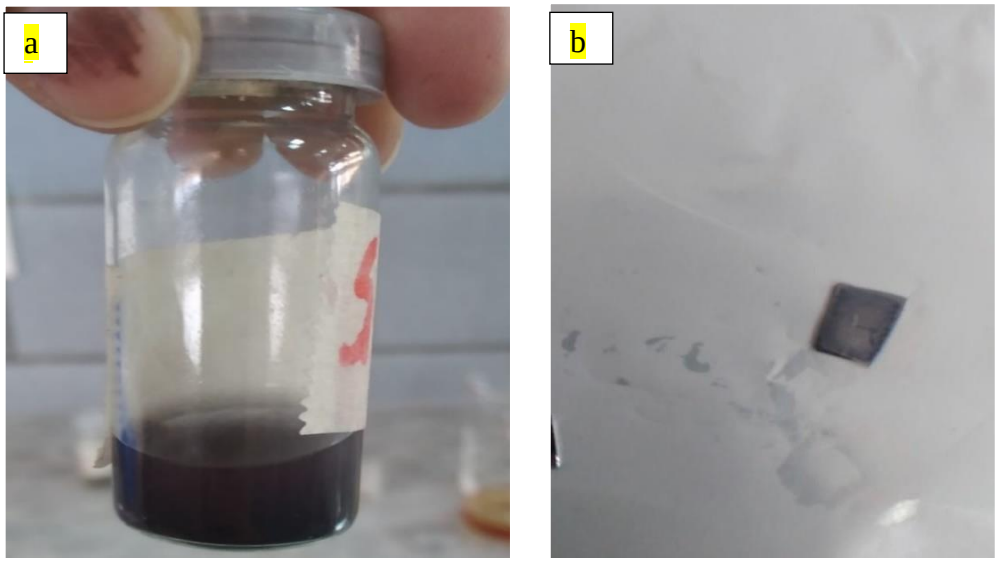

Fig 3.3: (a) solution after sonication **(b)** after drop casting of thin film

3.1 Characterization Techniques

The annealed thin films were characterized with various tools to study its structure, phase, and thermoelectric transport properties. To study the phase and structure of the samples, these thin films were characterized by XRD machine to obtain the corresponding XRD spectra and identify its structure and phase details.

The detail morphological investigation was carried out with the help of scanning electron microscope (SEM) and various morphologies of the SnSe2 structure were revealed. The absorption properties of the thin film Snse2 samples were studied with the help of Ultraviolet-visible (UV-Vis) spectrophotometry and Tauc plot analysis were carried out to find the optical band gap. Raman spectroscopic investigations were used to trace any impurity phases exists and to confirm the XRD investigations. For the thermoelectric analysis a custom lab scale designed thermoelectric setup was used to record the Seebeck and electrical resistivity from room temperature up to 675 K.

3.4.1 Scanning Electron Microscopy

Scanning electron microscopy is the major technique to determine the morphology, microstructure, shape, size, phase differences and surface topography of the sample material.

Scanning electron microscopy is a highly important characterization technique for investigation of size, morphology, microstructure, chemical composition, phase differences, surface topography and shape. It works by directing and focusing electron beam produce by heated filament source (gun), on surface of sample using objective and condenser lenses. The focused beam then interacts with a specific amount of sample either elastically or in-elastically.

Fig 3.4: Scanning Electron Microscope (SEM, Model JEOL JSM-64900)

As a result of this interaction, the result comes out in the form of morphology, external structure, chemical composition and crystalline structure. The elastic interaction tells us about the compositional differences and the inelastic interaction generates secondary electrons which can tell us about the surface of our sample. We used scanning electron microscope (SEM, Model JEOL JSM-64900) to analyze the different samples.

3.4.2 XRD

To find the crystallographic structure identification of different elements and identification of different compound, X- ray diffractometer was used. The working of XRD consists of X-ray tube. Generation of rays occur in X-ray tube and assemble towards the substrate or sample at the angle of θ. When the rays strike to the sample the diffraction occur from the crystal lattice and they interact with each other either constructively or destructively. The constructive interference tells us about the crystal structure. The crystal structure involves interatomic distances, position of atoms and atomic arrangement. This interference is based on Bragg's law. Bragg's law suggests that the path difference of X-rays is integral multiple of the incident wavelength.

$$n\lambda = 2d\sin\theta$$

where,

λ = wavelength

n = integer

d = spacing of path difference

θ = angle between the scattered plane and incident ray

The XRD graph is drawn between the intensity and the angle. The identification of XRD pattern is confirmed through the standard reference card. The crystalline structure shows from the peaks and the humps shows the amorphous sample. The width in the graph shows the microstructure.

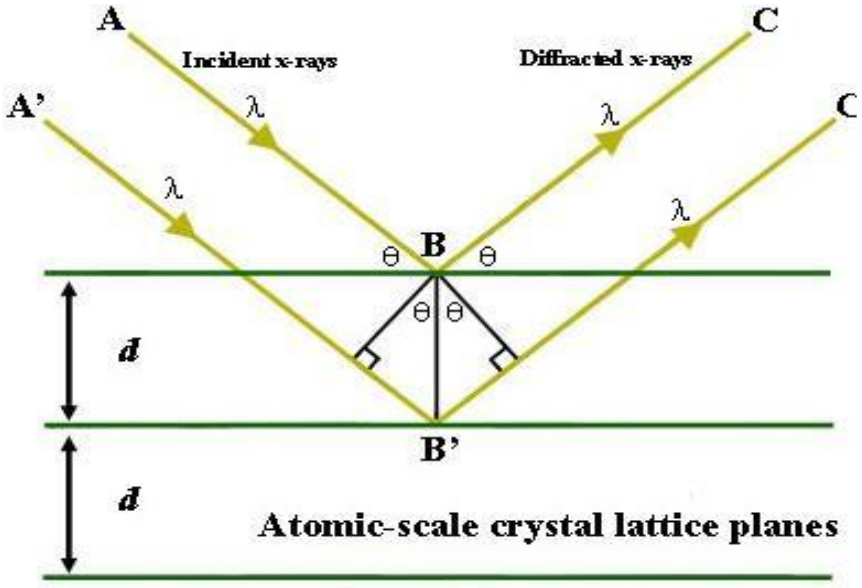

Fig 3.5: Bragg's Law

3.4.3 UV-VIS

Ultraviolet-Visible spectroscopy is basically absorption technique or reflectance technique in the ultraviolet and full visible region of the spectrum. Atoms and molecules go through electronic transition that take place in the ultraviolet and visible range. The basic principle of UV-VIS absorption is, molecules containing electrons that consume energy in the form of visible and ultraviolet light source, are used to stimulate the electrons towards the higher orbit. The electrons that are easily excited from lower energy band gap have a longer light absorption wavelength. When the light is passing through the sample the intensity is measured and then compared to the reference sample which in our case was ethanol.

The main parts of this instrument are the light source and holder that holds the sample, a prism and a detector. Tungsten filament is the source of radiations, and a deuterium arc lamp is also used. The detector used in this spectroscopy is basically photomultiplier tube.

The sample can be prepared in the form of suspension. Small amount of thick suspension is mixed in ethanol and transferred to the cuvettes. Then the cuvettes are placed in the instrument. One cuvette is placed as a reference sample.

Fig 3.6: UV-Visible spectroscopy

3.4.4 Raman spectroscopy

Raman spectroscopy is a non-destructive approach which can give us the information about the chemical structure, crystallinity and molecular interactions. It is the phenomena of light interaction with the chemical bonds within the deposited sample. Raman spectroscopy is called the light dispersion technique in which light source from high intensity falls on the sample and is scattered.

The scattered light that has the same wavelength as that of the incident light, it does not provide useful information and is called Rayleigh scattering. And the scattered light that has a different wavelength than the incident light is termed as Raman scattering and it

depends on the chemical structure. Raman spectra peaks tell us about the wavelength and intensity.

Raman spectroscopy gives us the information about chemical structure and identity, intrinsic stress/strain, contamination and impurity. This spectroscopy is used for microscopic analysis with resolution in order 0.5 to 1μm.

Fig 3.7: Raman spectroscopy

3.4.5 Hall Effect Measurements

In this method, samples are connected to a battery source, making a complete circuit. Electric current is then passed through this circuit and as a result of that, magnetic field is produced. A magnet is placed in the equipment and when the sample is brought near the magnet, a distortion in the magnetic field occurs. As a result of this distortion, the

carriers that were previously flowing along a linear path, now choose a certain direction where electrons flow to one side while the holes flow towards the other side. The deformation force is termed as Lorentz Force and the potential difference that is created is called hall voltage.

$$\mathbf{V_H} = \frac{IB}{\mathrm{q}nd}$$

V_H = Hall voltage

I = Current that flows to the circuit

B = Magnetic field

q = Charge in the circuit

n = Number of charges carries

d = thickness

Hall Effect is used for magnetic field sensing, used to measure the direct current, also used for phase angle measurement.

$$\mu = \frac{\sigma}{ne}$$

This is the Hall mobility.

Fig 3.8: Hall Effect Equipment

3.4.6 Thermoelectric properties

As we discussed these thermoelectric properties in the Chapter 1, here is a short overview on these TE properties. Using the required parameters, Power factor (PF) can be calculated. The required parameters for power factor are Seebeck coefficient and Electrical conductivity. The variation of Seebeck and Electrical conductivity with the variation in temperature helps us calculate PF at a wider temperature range; therefore, T is also used as one of the parameters.

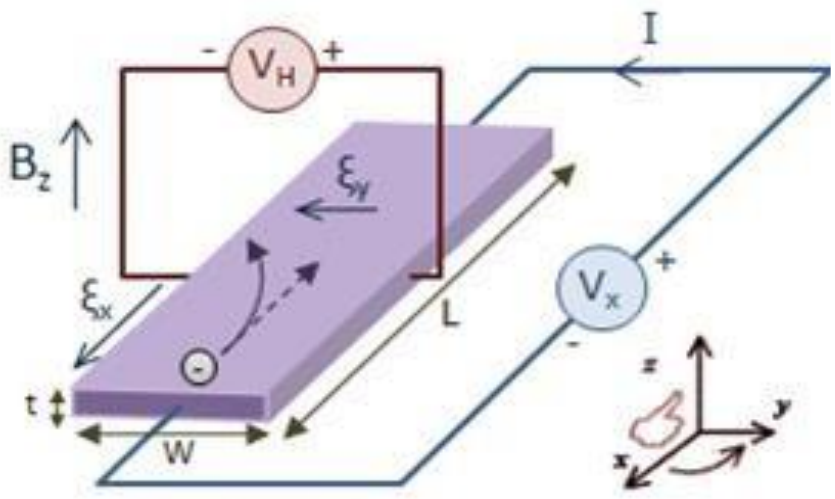

Fig 3.9 Schematic diagram of Hall Effect

The required parameters in TE are Seebeck coefficient and Electrical conductivity. The variation in Seebeck and Electrical conductivity is due to the variation in temperature that helps us to calculate PF at a wide temperature range; therefore, T is also used as one of the parameters.

Power factor is defined by formula

$$\mathbf{P.F} = S^2\sigma T$$

And to find the figure of merit ZT we require the power factor and thermal conductivity.

$$\mathbf{ZT} = \frac{P.F}{K}$$

High performance thermoelectric materials require higher ZT value. Custom designed TE Properties Apparatus was used to record the Seebeck and electrical resistivity with increasing temperature. The system was designed by the students of University of Oslo, Norway as can be seen in Figure 3.14. In this apparatus, the measurement cell is located in a vertical tubular furnace of 50cm length, fitted with the temperature controller. After placing the sample in the cell, the cell is sealed tightly in a quartz tube. The pressure enclosed in the measurement cavity is 1atm. The preferred composition in the chamber is measured by an in-house build gas mixer. The apparatus is optimized to measure disk

shape samples which are easiest to manufacture. In this apparatus, the TCs to be in direct interaction with the model, performing as both temperature and voltage probe. Overall three thermo couples are attached to the samples surface by spring loaded system to keep the TCs in the position. Springs are positioned at the end of the measurement chamber and not exposed to temperature significantly higher than of room temperature. One thermocouple placed at the bottom of the sample (TC1) and other thermocouples (TC2) and (TC3) is located above the sample with the distance $\sim 10mm$ above (TC2). Another Pt-wire is used being in direct connection with the surface sample. Thin thermocouple wires were used with the diameter of (0.2mm) to minimize the cold finger effect. On the other hand small contact area between sample and the TC result in the non-zero thermal resistance through the interfaces.

The equipment is attached with the two small Pt10Rh- coils below the TC1 and behind the TC2. These thermocouples act as internal heaters to fluctuate the temperature differences across the sample. These probes are used as a voltage measure and temperature measure. This phenomenon is called the van der Pauw method.

The Seebeck coefficient is obtained by the open circuit voltage that is formed due to the temperature differences.

$$a = \Delta U/\Delta T$$

In maximum setups the temperature difference ΔT IS altered with in a definite range and corresponding voltage is noted. For both in plane and cross-plane same procedure is adopted. The only difference occurs in the heating coil and the recording pair of thermocouples.

The conductivity of the disk shape sample can be obtained through a van der Pauw method. In case of bar sample the two thermocouples attached at the ends and serve as the current electrodes, whereas two extra platinum wires have to be attached to the sample to act as voltage probes.

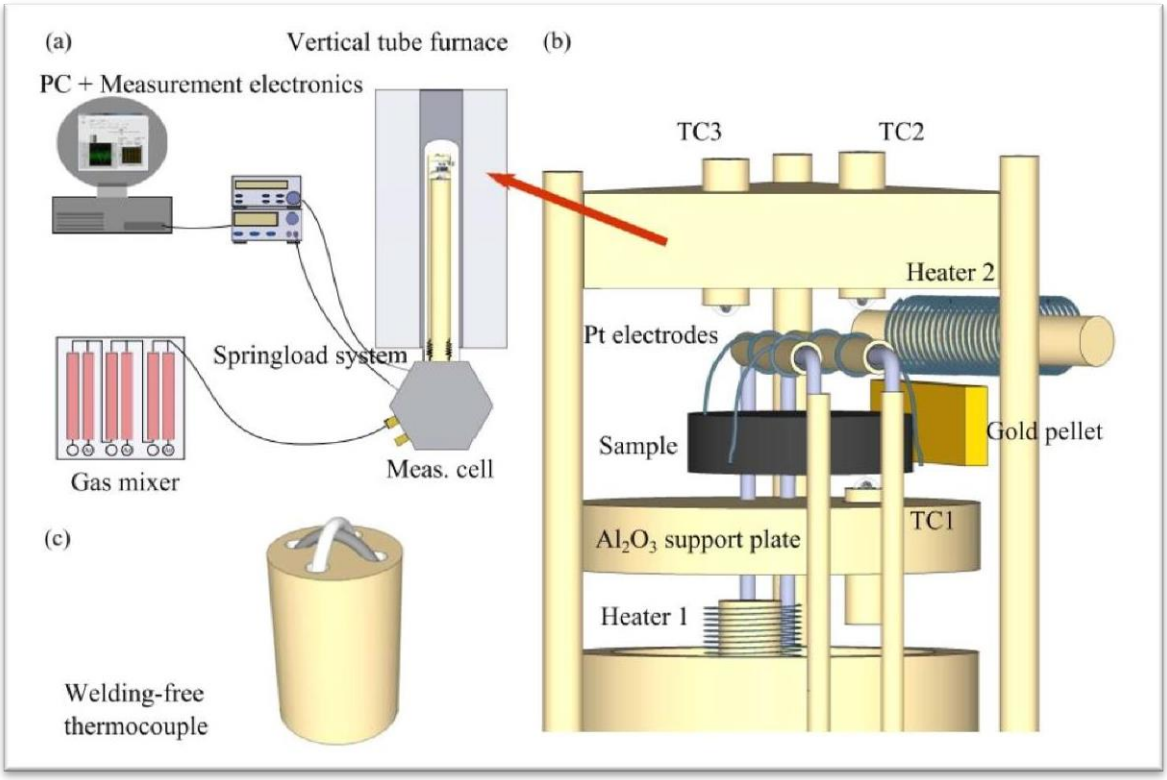

Figure 3.10: TE Measurement Apparatus

Chapter 4

Results and Discussion

4.1 Structural and Morphological studies

Figure 4.1 shows the XRD plot of Se and $SnSe_2$ Nano structured thin films of different four samples at the temperature of 180°C.

The XRD spectra of all the four samples, M1, M2, M3 and M4, are given in the Figure. 1. As we can see from these spectra that the snSe2 structures were successfully formed in all the fours samples along with small impurity phase of Selenium (Se). The presence of unreacted se is a common issue during synthesis of selenium based chalcogenides structures. Other findings which this XRD data reveals are that as we have increased the reaction time the amount of unreacted Se goes down and more pure structure of SnSe2 was obtained.

The intense sharp peaks are indication of fine crystal structure of $SnSe_2$. The broad humps in the XRD pattern show the amorphous nature of the sample. The M4 sample peaks are more accurate and sharp and show the pure Se and $SnSe_2$ crystal structure.

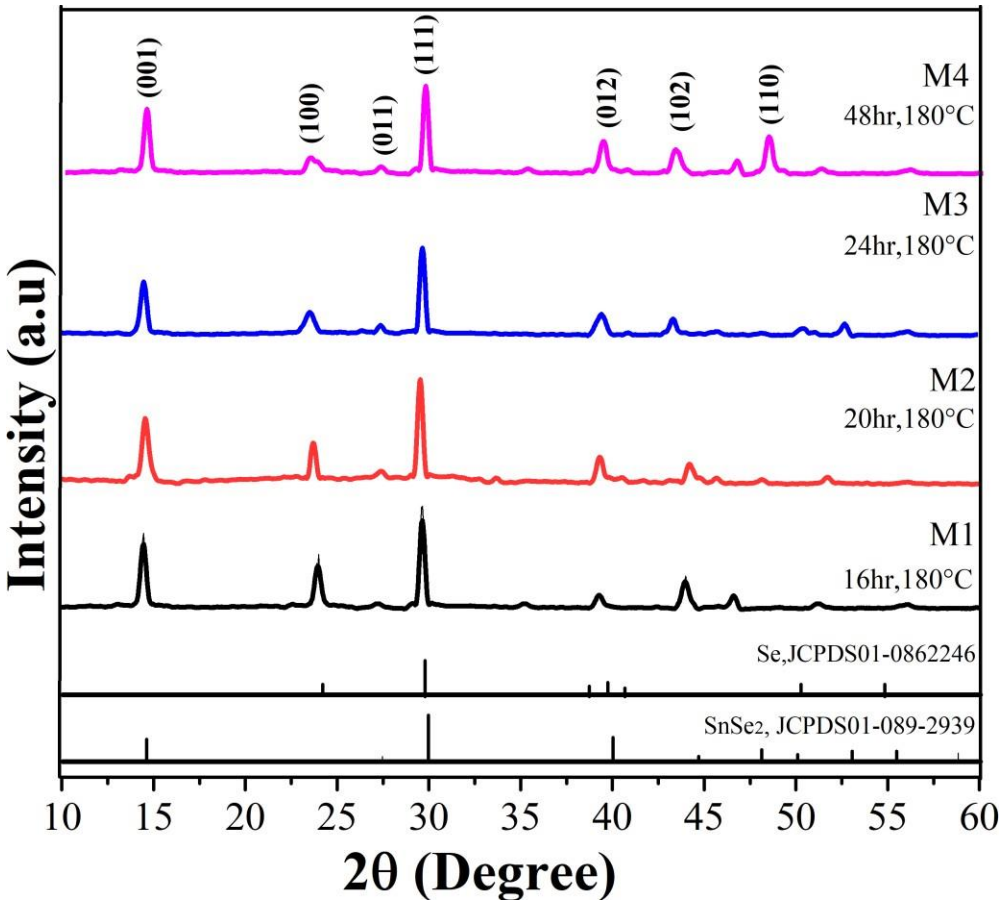

Figure 4. 1 The XRD spectra of all the four samples, M1, M2, M3 and M4. The detail of different samples along with reaction time and temperature is given.

4.2 Scanning Electron Microscopy (SEM analysis)

Morphological control via different reaction time and its effect on the thermoelectric properties was the motive behind our study. Figure.3 shows the SEM images of $SnSe_2$ thin films annealed at 300 °C for 30 minutes in the presence of nitrogen. Figure. 3a shows that theoverall morphology of the sample consists of irregular agglomerates with few elongated structures. Figure. 3b shows that with the increase of reaction time from 16 to 20 hours the agglomerated types of structures start to elongate in form of rod type morphology. With further increase of reaction time at 24 hours, mix morphology consists of flowers and rods can be easily identified from the SEM micrograph Figure 3c.

When thereaction time was increased up to 48 hours, flowers type morphology was become dominant as shown in Figure. 3d. the presence of rods are actually unreacted Se which are grown in form of rods type morphology and it is confirmed from XRD results that with increasing time the amount of Se going to be reduced. This argument may well be supported with the help of Raman analysis where the peaks at 240 cm^{-1} in M1, gradually moves towards left which shows the reduction of Se amount present which in turn enhance the phase purity of the SnSe2 structure.

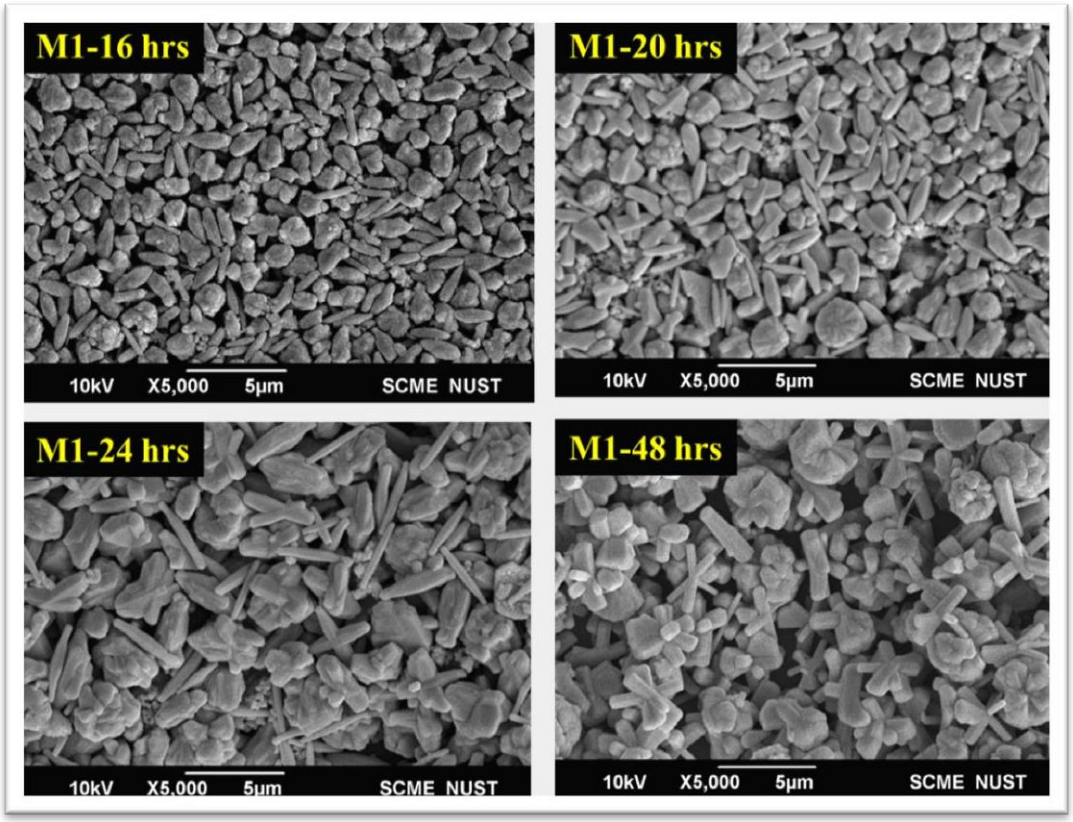

Figure.4.2 $SnSe_2$ thin films obtained by drop casting of the thick solution on the glass substrate. The different morphological structures can be identified from these micrographs.

4.3 Raman Spectroscopy analysis

Raman spectroscopy was used to look for any impurity present in the $SnSe_2$ structure and confirm the XRD findings of $SnSe_2$ nano structured thin films shown in Figure. 2.

The characterstic spectra was recorded at room temperature in the range of raman shift from 50 to 350 cm^{-1} while the exciting photon energy was 2.41ev. These peaks were achived by using the laser excitation wavelength is 532 nm. The first peak indicate the Eg mode which is almost at 148.6 cm^{-1} and the second peak corrosponding to the A1g mode is the wide peak at around 240 cm^{-1} for the M1sample. The actual positions of pure $SnSe_2$ Raman shifts are around 115 cm^{-1} and 170 cm^{-1} respectively as obtained for the sample M4. The overall spectra shifts towards lower values of the Raman shift as the reaction time was increased and the Raman shifts alligned more with the pure $SnSe_2$ Raman spectra. From these observations it can be concluded that at low reaction time some unreacted Se was present in the samples , which has been decreased with increasing reaction time. The Raman results supports the overall XRD analysis

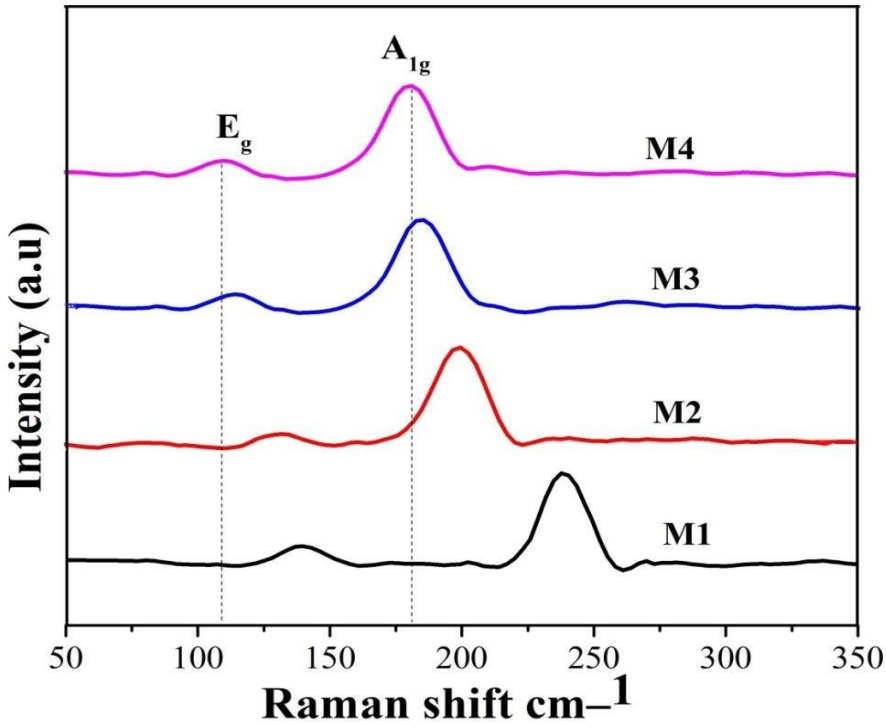

Figure 4.3 Raman spectroscopic analysis of the four samples M1, M2 M3 and M4 from 50 to 350 Raman Shift.

4.4 UV-Visible Spectroscopy Analysis

The optical analysis of deposited $SnSe_2$ thin film can be measured from the wavelength range of 300 to 2400 nm by using UV-Visible spectrometer. Figure 4.4 shows the graph between wavelength and absorbance spectra. The graph shows that the $SnSe_2$ film grows at 180°C temperature. The M1 shows the lesser absorbance than the M4 by varying heat treatment time.

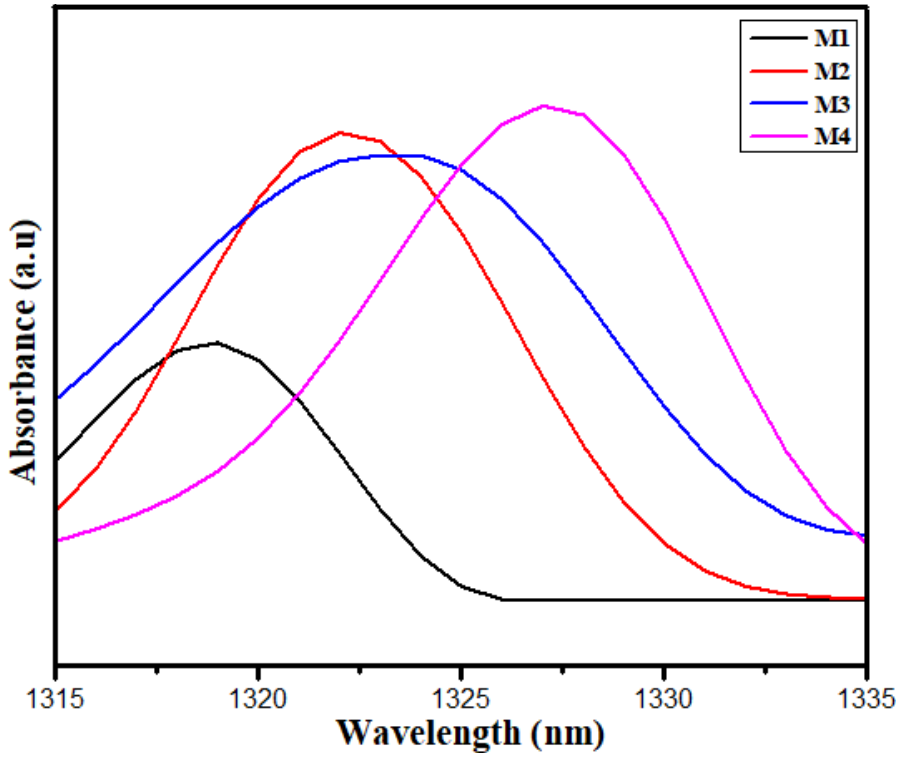

Fig 4.4: absorption curve of $SnSe_2$ thin film

The absorption coefficient α can be expressed in the equation

$$a = \frac{2.303(A)}{t}$$

$$\alpha hu = \mathrm{A}\ (hu - E_g)^{n}$$

t is the thickness of sample and A is the absorbance while Eg represent the optical band gap of the sample, *hu* is the energy of the photon and n represent the transition while A is absorption constant. The optical band gap is usually obtained with the help of the Tauc plotting.

The calculated band gap values of the $SnSe_2$ thin film samples from the absorption data and Tauc plot are shown in the Figure. 4.4. Usually the band gap value is taken as the intercept extended from the hump of the Tauc plot spectra to the X-axis as show in the Figure 4.5. The band gap analysis reveals that with increasing reaction time morphological changes were resulted which further changes the band gap values and hence the electronic transport properties were also affected. As we can see from the figure 4.5 that with increasing reaction time the band gap of the sample M4 is going to shrink compare to the sample M1. These findings are very helpful to further

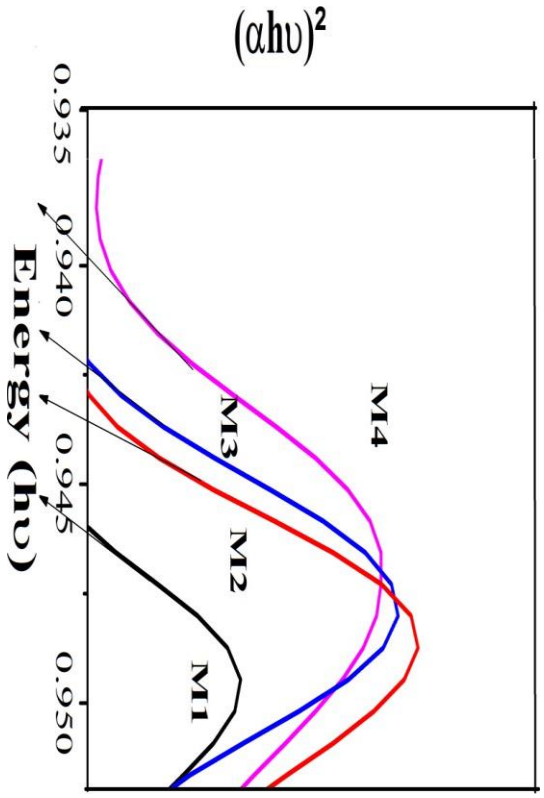

understand the thermal and electronic transport properties of the SnSe2 structure.

Fig 4.4: Energy Band gap

.

4.5 Hall measurement

Hall measurement is done at different temperatures from 300k to 680k. The method is used for hall measurement is vender Pauw method and the magnetic field is reversible of

0.7T. Table shows the temperature dependent of carrier concentration n (T) that values are obtained from hall measurement. Formula that is used in hall measurement is

$$\frac{VH}{I} = \frac{1}{ned}\mathrm{H}$$

Where V_H is the Hall voltage, n number of carriers, I is the current, e is the electric charge, d sample thickness, H is hall magnetic field.

In table clearly shows that as increasing temperature the value of carrier concentration increases. In the sample M1 the value of carrier concentration increases at 300k to 675k with the concentration value 1.39* $10^8 cm^{-3}$to 26.79* $10^8 cm^{-3}$. The carrier mobility is decrease as carrier concentration increase the reason behind this is the acoustic phonon scattering.

The table shows the hall measurement values of four samples at different time of heat treatment.

Table 4.1: Hall measurements at Room Temperature

Sample	Carrier Concentration (n)$10^8 cm^{-3}$	Carrier mobility μ (cm^2/v.s)
M1	1.39×10^{18}	41.95
M2	1.53×10^{18}	40.03
M3	1.61×10^{18}	38.19
M4	1.80×10^{18}	35.30

4.6 Thermoelectric Properties

Thermoelectric materials convert heat into electricity and come up with the possible solution for the energy crisis in the world. We study the thermoelectric properties parallel to the plan. The sample must be in bar shaped is used to measure the Seebeck, electrical conductivity and power factor. Electrical conductivity and Seebeck coefficient is measured in Argon environment is to avoid the oxidation and evaporation. Some of the achievements in thermoelectric properties are texturing, hole doping and

Microstructures can be obtained in TE properties. In thermoelectric properties different parameters involved Seebeck, electrical conductivity power factor, thermal conductivity and the most important figure of merit value. We will start with the electrical conductivity graph.

The behavior of the electrical conductivity (σ) for the four SnSe2 samples can easily be understood with the help of band gap data in Figure 4.5. The temperature based electrical conductivity data is given in Figure. 6 (a). Here it is noticeable that as we increase the temperature the σ going to decrease. This type of behavior is metallic type nature with high carrier concentration. Further it can be seen from the same figure that The overall all temperature values of σ are relatively higher for M4 sample than M1.

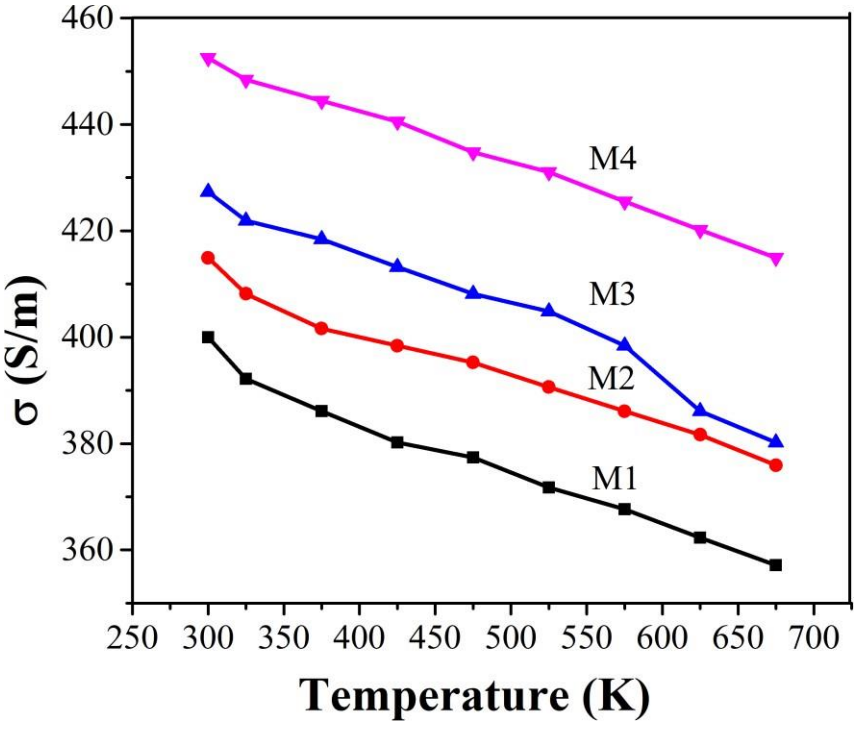

Fig 4.6(a): Electrical conductivity data of the $SnSe_2$ samples

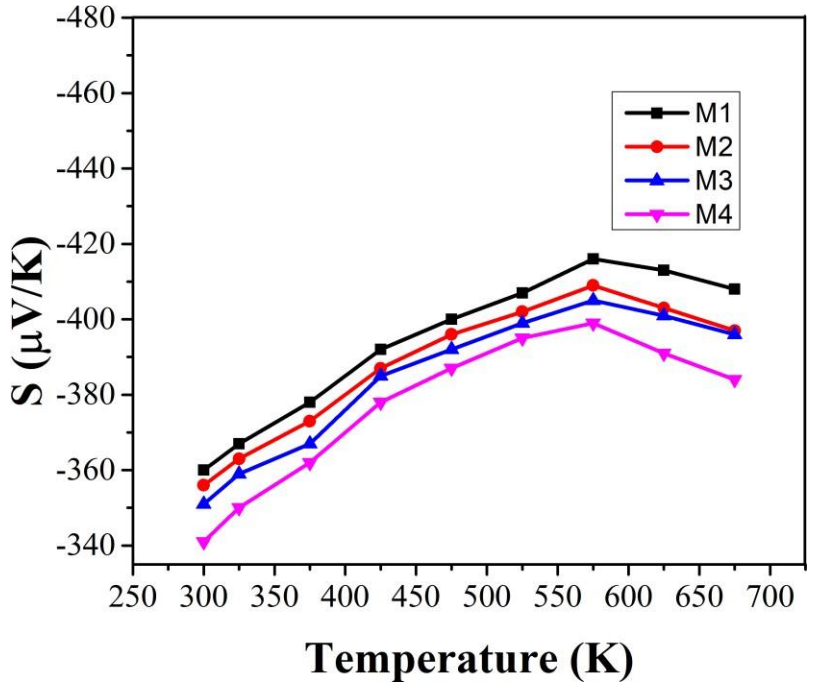

4.6(b): Temperature dependent Seebeck coefficient data for the four samples

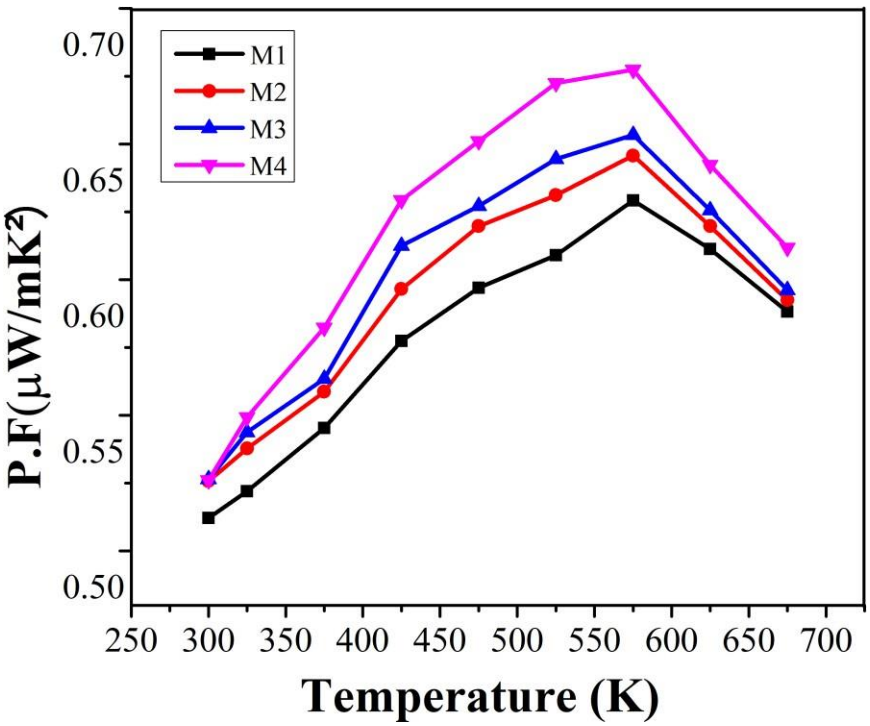

4.6(c): Power factor
Values calculated from the electrical conductivity and Seebeck data.

This data can be related to the band gap values of these samples. With increasing reaction time the change in flower like morphology may leads to band gap lowering which further enhance the σ values respectively.

Similarly the Seebeck (S) values are given in Figure 4.6 (b) which is again in agreement with the electronic properties of the $SnSe_2$ samples. With increasing measurement temperature the S values for all the samples are going to increase up to 570 K. after 570 K the fall of S values for the entire four samples can be noticed which actually the result of bipolar effect is. At some high temperature the bipolar effect is activated in these chalcogenides where low energy carriers start to take part in the electronic transport of the structure. Due to these low energy carriers the overall S values are negatively affected. More over the negative S values of all the studied samples reveals the n-type electronic transport nature of the $SnSe_2$. Although the S values for the studied samples are good but still the overall power factor values of these sample are not that much good enough. The reason behind this is the compromised values σ. The peak value of power factor we have obtained is for M4 sample at around 0.69 $\mu Wm^{-1}K^{-2}$ for peak temperature at 580 K as shown in Figure 6d.

The observed thermoelectric properties are in good range of already reported related literature. The final findings of the study is that with increasing reaction time flower like morphology was obtained where low band gap values were resulted and hence slightly improved the thermoelectric performance of the $SnSe_2$ structure.

Conclusion

We have successfully synthesized $SnSe_2$ structure with different morphologies via solvothermal route and obtained somehow control over its morphology by varying the reaction time. The solvothermal synthesis route was selected due its better control on morphology and microstructure. We have studied the thermoelectric properties of the $SnSe_2$ samples and found that morphology and phase purity can affect thermoelectric performance of the structure. The comparatively larger power factor value of the sample M4 can be related to the increase in its electrical conductivity due to increase in phase purity and band gap reduction. The summary of the study is that with increasing reaction time flower like morphology was obtained where low band gap values were resulted and hence slightly improved the thermoelectric performance of the $SnSe_2$ structure.

References

[1] Chen, Z., Han, G., Yang, L., Cheng, L., & Zou, J. (2012). Nanostructured thermoelectric materials: Current research and future challenge. *Progress in Natural Science: Materials International, 22*(6), 535-549. doi:10.1016/j.pnsc.2012.11.011

[2] Singh, N. K., Bathula, S., Gahtori, B., Tyagi, K., Haranath, D., & Dhar, A. (2016). The effect of doping on thermoelectric performance of p-type SnSe: Promising thermoelectric material. *Journal of Alloys and Compounds, 668*, 152-158. doi:10.1016/j.jallcom.2016.01.190

[3] Liu, W., Hu, J., Zhang, S., Deng, M., Han, C., & Liu, Y. (2017). New trends, strategies and opportunities in thermoelectric materials: A perspective. *Materials Today Physics, 1*, 50-60. doi:10.1016/j.mtphys.2017.06.001

[4] Ding, G., Hu, Y., Li, D., & Wang, X. (2019). A comparative study of thermoelectric properties between bulk and monolayer SnSe. *Results in Physics, 15*, 102631. doi:10.1016/j.rinp.2019.102631

[5] Shi, X., Chen, Z., Liu, W., Yang, L., Hong, M., Moshwan, R., Zou, J. (2018). Achieving high Figure of Merit in p-type polycrystalline Sn0.98Se via self-doping and anisotropy-strengthening. *Energy Storage Materials, 10*, 130-138. doi:10.1016/j.ensm.2017.08.014

[6] Junior, O. A., Maran, A., & Henao, N. (2018). A review of the development and applications of thermoelectric microgenerators for energy harvesting. *Renewable and Sustainable Energy Reviews, 91*, 376-393. doi:10.1016/j.rser.2018.03.052

[7] Sajid, M., Hassan, I., & Rahman, A. (2017). An overview of cooling of thermoelectric devices. *Renewable and Sustainable Energy Reviews, 78*, 15-22. doi:10.1016/j.rser.2017.04.098

[8] Zuhud, A. M., Mochammad, F., & Widayat, W. (2018). Thermoelectric application in energy conservation. *E3S Web of Conferences, 73*, 01009. doi:10.1051/e3sconf/20187301009

[9] Shi, X., Chen, L., & Uher, C. (2016). Recent advances in high-performance bulk thermoelectric materials. *International Materials Reviews, 61*(6), 379-415. doi:10.1080/09506608.2016.1183075

[10] Date, A., Date, A., Dixon, C., & Akbarzadeh, A. (2014). Progress of thermoelectric power generation systems: Prospect for small to medium scale power generation. *Renewable and Sustainable Energy Reviews, 33*, 371-381. doi:10.1016/j.rser.2014.01.081

[11] Brignone, M., & Ziggiotti, A. (2012). Impact of novel thermoelectric materials on automotive applications. doi:10.1063/1.4731601

[12] Wang, Z., Leonov, V., Fiorini, P., & Hoof, C. V. (2009). Realization of a wearable miniaturized thermoelectric generator for human body applications. *Sensors and Actuators A: Physical, 156*(1), 95-102. doi:10.1016/j.sna.2009.02.028

[13] Liu, H., Wang, Y., Mei, D., Shi, Y., & Chen, Z. (2016). Design of a Wearable Thermoelectric Generator for Harvesting Human Body Energy. *Wearable Sensors and Robots Lecture Notes in Electrical Engineering,* 55-66. doi:10.1007/978-981-10-2404-7_5

[14] Kumar, S., Heister, S. D., Xu, X., Salvador, J. R., & Meisner, G. P. (2013). Thermoelectric Generators for Automotive Waste Heat Recovery Systems Part I: Numerical Modeling and Baseline Model Analysis. *Journal of Electronic Materials, 42*(4), 665-674. doi:10.1007/s11664-013-2471-9

[15] Dresselhaus, M. S., Chen, G., Tang, M. Y., Yang, R., Lee, H., Wang, D., . . . Gogna, P. (2007). New Directions for Low-Dimensional Thermoelectric Materials. *ChemInform, 38*(26). doi:10.1002/chin.200726202

[16] Liu, W., Yan, X., Chen, G., & Ren, Z. (2012). Recent advances in thermoelectric nanocomposites. *Nano Energy, 1*(1), 42-56. doi:10.1016/j.nanoen.2011.10.001

[17] Guzowski, B., Gozdur, R., & Lakomski, M. (2018). Thermoelectric Generation Based on Spin Seebeck Effect in NiFeCuMo Alloy. *Acta Physica Polonica A, 133*(3), 541-543. doi:10.12693/aphyspola.133.541

[18] Eslamian, M., & Soltani-Kordshuli, F. (2017). Development of multiple-droplet drop-casting method for the fabrication of coatings and thin solid films. *Journal*

of Coatings Technology and Research, 15(2), 271-280. doi:10.1007/s11998-017-9975-9

[19] Kumar, A. K., Zhang, Y., Li, D., & Compton, R. G. (2020). A mini-review: How reliable is the drop casting technique? *Electrochemistry Communications, 121*, 106867. doi:10.1016/j.elecom.2020.106867

[20] Liu, Y., Zhao, X., Cai, B., Pei, T., Tong, Y., Tang, Q., & Liu, Y. (2014). Controllable fabrication of oriented micro/nanowire arrays of dibenzo-tetrathiafulvalene by a multiple drop-casting method. *Nanoscale, 6*(3), 1323-1328. doi:10.1039/c3nr05680e

[21] Conventional Optimization Techniques for Manufacturing Applications. (2006). *Manufacturing Optimization through Intelligent Techniques*, 27-40. doi:10.1201/b16949-7

[22] Liu, X. (n.d.). High-Performance Bi2Te3-Based Thermoelectric Materials: Fundamentals, Fabrication, and Characterisation. doi:10.14264/uql.2018.293

[23] Boyer, A., & Cissé, E. (1992). Properties of thin film thermoelectric materials: Application to sensors using the Seebeck effect. *Materials Science and Engineering: B, 13*(2), 103-111. doi:10.1016/0921-5107(92)90149-4

[24] Jia, B., Liu, S., Li, G., Liu, S., Zhou, Y., & Wang, Q. (2019). Study on thermoelectric properties of co-evaporated Sn-Se films with different phase formations. *Thin Solid Films, 672*, 133-137. doi:10.1016/j.tsf.2019.01.017

[25] Caroff, T., Sarno, C., Hodot, R., Brignone, M., & Simon, J. (2015). New Optimization Strategy of Thermoelectric Coolers Applied to Automotive and Avionic Applications. *Materials Today: Proceedings, 2*(2), 751-760. doi:10.1016/j.matpr.2015.05.095

[26] Belov, I., Volkov, V., & Manyakin, O. (n.d.). Optimization of Peltier thermocouple using distributed Peltier effect. *Eighteenth International Conference on Thermoelectrics. Proceedings, ICT99 (Cat. No.99TH8407)*. doi:10.1109/ict.1999.843392

[27] Jin, W., Liu, L., Yang, T., Shen, H., Zhu, J., Xu, W., . . . Zhu, D. (2018). Exploring Peltier effect in organic thermoelectric films. *Nature Communications, 9*(1). doi:10.1038/s41467-018-05999-4

[28] Huang, M., Yen, R., & Wang, A. (2005). The influence of the Thomson effect on the performance of a thermoelectric cooler. *International Journal of Heat and Mass Transfer, 48*(2), 413-418. doi:10.1016/j.ijheatmasstransfer.2004.05.040

[29] Lashkevych, I., Velázquez, J. E., Titov, O. Y., & Gurevich, Y. G. (2018). Special Important Aspects of the Thomson Effect. *Journal of Electronic Materials, 47*(6), 3189-3192. doi:10.1007/s11664-018-6205-x

[30] Snyder, G. J., & Snyder, A. H. (2017). Figure of merit ZT of a thermoelectric device defined from materials properties. *Energy & Environmental Science, 10*(11), 2280-2283. doi:10.1039/c7ee02007d

[31] Baliga, B. (1989). Power semiconductor device figure of merit for high-frequency applications. *IEEE Electron Device Letters, 10*(10), 455-457. doi:10.1109/55.43098

[32] Haacke, G. (1976). New figure of merit for transparent conductors. *Journal of Applied Physics, 47*(9), 4086-4089. doi:10.1063/1.323240

[33] Meng, B., Liu, J., & Wang, L. (2021). Recent development of n-type thermoelectric materials based on conjugated polymers. *Nano Materials Science, 3*(2), 113-123. doi:10.1016/j.nanoms.2020.10.002

[34] Masood, K. B., Kumar, P., Singh, R. A., & Singh, J. (2018). Odyssey of thermoelectric materials: Foundation of the complex structure. *Journal of Physics Communications, 2*(6), 062001. doi:10.1088/2399-6528/aab64f

[35] Xu, P., Fu, T., Xin, J., Liu, Y., Ying, P., Zhao, X., . . . Zhu, T. (2017). Anisotropic thermoelectric properties of layered compound SnSe 2. *Science Bulletin, 62*(24), 1663-1668. doi:10.1016/j.scib.2017.11.015

[36] Li, C., He, W., Wang, D., & Zhao, L. (2021). Investigations on the anisotropic thermoelectric transport properties in polycrystalline SnSe2. *Chinese Physics B*. doi:10.1088/1674-1056/abeee1

[37] Yang, C. C., & Li, S. (2011). Basic Principles for Rational Design of High-Performance Nanostructured Silicon-Based Thermoelectric Materials. *ChemPhysChem, 12*(18), 3614-3618. doi:10.1002/cphc.201100514

[38] Yamamoto, A., & Ohta, T. (n.d.). Thermoelectric figure of merit of silicide two-dimensional quantum wells. *IECEC 96. Proceedings of the 31st Intersociety Energy Conversion Engineering Conference*. doi:10.1109/iecec.1996.553819

[39] Zhang, X., & Zhao, L. (2015). Thermoelectric materials: Energy conversion between heat and electricity. *Journal of Materiomics, 1*(2), 92-105. doi:10.1016/j.jmat.2015.01.001

[40] Wei, T., Wu, C., Li, F., & Li, J. (2018). Low-cost and environmentally benign selenides as promising thermoelectric materials. *Journal of Materiomics, 4*(4), 304-320. doi:10.1016/j.jmat.2018.07.001

[41] Jung, Y., Zhou, Y., & Cha, J. J. (2016). ChemInform Abstract: Intercalation in Two-Dimensional Transition Metal Chalcogenides. *ChemInform, 47*(26). doi:10.1002/chin.201626221

[42] Xia, C., & Li, J. (2016). Recent advances in optoelectronic properties and applications of two-dimensional metal chalcogenides. *Journal of Semiconductors, 37*(5), 051001. doi:10.1088/1674-4926/37/5/051001

[43] Bletskan, D. (2016). Electronic structure of 2H-SnSe2: Ab initio modeling and comparison with experiment. *Semiconductor Physics Quantum Electronics and Optoelectronics, 19*(1), 98-108. doi:10.15407/spqeo19.01.098

[44] Transport Properties and High Thermopower of SnSe2: A Full Ab-Initio Investigation. (n.d.). doi:10.1021/acs.jpcc.6b11467.s001

[45] Pei, Y., Wang, H., & Snyder, G. J. (2012). Thermoelectric Materials: Band Engineering of Thermoelectric Materials (Adv. Mater. 46/2012). *Advanced Materials, 24*(46), 6124-6124. doi:10.1002/adma.201290290

[46] Li, C., He, W., Wang, D., & Zhao, L. (2021). Investigations on the anisotropic thermoelectric transport properties in polycrystalline SnSe2. *Chinese Physics B*. doi:10.1088/1674-1056/abeee1

[47] Jalil, O., Ahmad, S., Liu, X., Ang, K. W., & Younis, U. (2020). Towards theoretical framework for probing the accuracy limit of electronic transport properties of SnSe2 using many-body calculations. *EPL (Europhysics Letters), 130*(5), 57001. doi:10.1209/0295-5075/130/57001

[48] Transport Properties and High Thermopower of SnSe2: A Full Ab-Initio Investigation. (n.d.). doi:10.1021/acs.jpcc.6b11467.s001

[49] Chen, J., Hamann, D. M., Choi, D., Poudel, N., Shen, L., Shi, L., . . . Cronin, S. (2018). Enhanced Cross-Plane Thermoelectric Transport of Rotationally Disordered SnSe2 via Se-Vapor Annealing. *Nano Letters, 18*(11), 6876-6881. doi:10.1021/acs.nanolett.8b02744

[50] Pham, A., Vu, T. H., Cheng, C., Trinh, T. L., Lee, J., Ryu, H., . . . Cho, S. (2020). High-Quality SnSe2 Single Crystals: Electronic and Thermoelectric Properties. *ACS Applied Energy Materials, 3*(11), 10787-10792. doi:10.1021/acsaem.0c01846

[51] Hadland, E., Jang, H., Falmbigl, M., Fischer, R., Medlin, D. L., Cahill, D. G., & Johnson, D. C. (2019). Synthesis, Characterization, and Ultralow Thermal Conductivity of a Lattice-Mismatched SnSe2(MoSe2)1.32 Heterostructure. *Chemistry of Materials, 31*(15), 5699-5705. doi:10.1021/acs.chemmater.9b01637

[52] Shafique, A., Samad, A., & Shin, Y. (2017). Ultra low lattice thermal conductivity and high carrier mobility of monolayer SnS2and SnSe2: A first principles study. *Physical Chemistry Chemical Physics, 19*(31), 20677-20683. doi:10.1039/c7cp03748a

[53] Cao, L., Pan, J., Zhang, H., Zhang, Y., Wu, Y., Lv, Y., . . . Chen, Y. (2019). One-Order Decreased Lattice Thermal Conductivity of SnSe Crystals by the Introduction of Nanometer SnSe2 Secondary Phase. *The Journal of Physical Chemistry C, 123*(45), 27666-27671. doi:10.1021/acs.jpcc.9b08700

[54] Lee, M., Ahn, J., Sung, J. H., Heo, H., Jeon, S. G., Lee, W., Jo, M. (2016). Thermoelectric materials by using two-dimensional materials with negative correlation between electrical and thermal conductivity. *Nature Communications, 7*(1). doi:10.1038/ncomms12011

[55] Chen, X., Dai, W., Wu, T., Luo, W., Yang, J., Jiang, W., & Wang, L. (2018). Thin Film Thermoelectric Materials: Classification, Characterization, and Potential for Wearable Applications. *Coatings, 8*(7), 244. doi:10.3390/coatings8070244

[56] Zhang, Y., Hao, S., Zhao, L., Wolverton, C., & Zeng, Z. (2016). Pressure induced thermoelectric enhancement in SnSe crystals. *Journal of Materials Chemistry A, 4*(31), 12073-12079. doi:10.1039/c6ta03625b

[57] Okazaki, A., & Ueda, I. (1956). The Crystal Structure of Stannous Selenide SnSe. *Journal of the Physical Society of Japan, 11*(4), 470-470. doi:10.1143/jpsj.11.470

[58] Afrin, S. (2000). Investigation of Electronic and Optical Properties of 2-Dimensional Semiconductor Tin Selenide (SnSe) Thin Films. doi:10.15760/etd.6738

[59] Lochocki, E. B., Vishwanath, S., Liu, X., Dobrowolska, M., Furdyna, J., Xing, H. G., & Shen, K. M. (2019). Electronic structure of SnSe2 films grown by molecular beam epitaxy. *Applied Physics Letters, 114*(9), 091602. doi:10.1063/1.5084147

[60] Saritha, K., Reddy, G. P., & Reddy, K. R. (2016). Studies on Physical Properties of SnSe2 Thin Films Grown by a Two-Stage Process. *Materials Today: Proceedings, 3*(10), 4128-4133. doi:10.1016/j.matpr.2016.11.085

[61] Martínez-Escobar, D., Ramachandran, M., Sánchez-Juárez, A., & Rios, J. S. (2013). Optical and electrical properties of SnSe2 and SnSe thin films prepared by spray pyrolysis. *Thin Solid Films, 535*, 390-393. doi:10.1016/j.tsf.2012.12.081

[62] Sharma, J., Singh, R., Singh, H., Singh, T., Singh, P., Thakur, A., & Tripathi, S. (2017). Synthesis of SnSe2 thin films by thermally induced phase transition in SnSe. *Journal of Alloys and Compounds, 724*, 62-66. doi:10.1016/j.jallcom.2017.06.344

[63] Saritha, K., Reddy, G. P., & Reddy, K. R. (2016). Studies on Physical Properties of SnSe2 Thin Films Grown by a Two-Stage Process. *Materials Today: Proceedings, 3*(10), 4128-4133. doi:10.1016/j.matpr.2016.11.085

[64] Barrios-Salgado, E., Nair, M., & Nair, P. (2016). Thin films of n-type SnSe2 produced from chemically deposited p-type SnSe. *Thin Solid Films, 598*, 149-155. doi:10.1016/j.tsf.2015.11.075

[65] Chen, H., Jia, B., Lu, X., Guo, Y., Hu, R., Khatoon, R., . . . Lu, J. (2019). Two-Dimensional SnSe 2 /CNTs Hybrid Nanostructures as Anode Materials for High- Performance Lithium- Ion Batteries. *Chemistry – A European Journal, 25*(42), 9973-9983. doi:10.1002/chem.201901487

[66] Fang, Z., Hao, S., Long, L., Fang, H., Qiang, T., & Song, Y. (2014). The enhanced photoelectrochemical response of SnSe2 nanosheets. *CrystEngComm, 16*(12), 2404. doi:10.1039/c3ce42082e

[67] Chen, H., Guo, Y., Ma, P., Hu, R., Khatoon, R., Lu, Y., . . . Lu, J. (2019). Hydrothermal synthesis of Cu-doped SnSe2 nanostructure for efficient lithium storage. *Journal of Electroanalytical Chemistry, 847*, 113205. doi:10.1016/j.jelechem.2019.113205

[68] Liu, K., Liu, H., Wang, J., & Feng, L. (2009). Synthesis and characterization of SnSe2 hexagonal nanoflakes. *Materials Letters, 63*(5), 512-514. doi:10.1016/j.matlet.2008.10.054

[69] Duong, A. T., Nguyen, D. L., Nguyen, M. N., Nguyen, T. M., Nguyen, A. D., Pham, A. T., ... Cho, S. (2019). High thermoelectric power factor in SnSe2 thin film grown on Al2O3 substrate. *Materials Research Express, 6*(6), 066420. doi:10.1088/2053-1591/ab1031

[70] Zhao, D., & Tan, G. (2014). A review of thermoelectric cooling: Materials, modeling and applications. *Applied Thermal Engineering, 66*(1-2), 15-24. doi:10.1016/j.applthermaleng.2014.01.074

[71] Yin, Y., Tudu, B., & Tiwari, A. (2017). Recent advances in oxide thermoelectric materials and modules. *Vacuum, 146*, 356-374. doi:10.1016/j.vacuum.2017.04.015s

v